THESIS

EFFECTS OF MOUNTAIN PINE BEETLE CAUSED TREE MORTALITY ON STREAMFLOW AND STREAMFLOW GENERATION MECHANISMS IN COLORADO

Submitted by

Ariann Lenore Maggart

Department of Ecosystem Science and Sustainability

In partial fulfillment of the requirements

For the Degree of Master of Science

Colorado State University

Fort Collins, Colorado

Spring 2014

Master's Committee:

Advisor: John D. Stednick

Steven Fassnacht
Michael Ronayne

ABSTRACT

EFFECTS OF MOUNTAIN PINE BEETLE CAUSED TREE MORTALITY ON STREAMFLOW AND STREAMFLOW GENERATION MECHANISMS IN COLORADO.

The mountain pine beetle (*Dendroctonus ponderosae* Hopkins) (MPB), an endemic beetle in Colorado forests, saw dramatic population growth in the 1990's. As a result of this epidemic, the mountain pine beetle killed large tracts of forest as it spread. To evaluate the effects of MPB caused tree mortality on streamflow and streamflow generation mechanisms multiple investigative approaches were taken. In north-central Colorado, 21 watersheds representing minimally to highly affected watershed areas were chosen. Physical watershed characteristics were determined through a geographic information system. Long-term streamflow records for each watershed were assessed for data stationarity and change-points in peak flow, date of peak flow and annual water yield. Peak streamflow, date of peak streamflow and annual water yield all had stationarity. Since data were stationary, change-point analyses were not conducted. Streamflow, groundwater and precipitation samples were collected and analyzed for stable isotope concentrations. Isotopes of ^{2}H and ^{18}O partition source water contributions to streamflow from precipitation as snow or rain and groundwater (as a surrogate for groundwater).

Annual $\delta^{2}H$ and $\delta^{18}O$ isotopic signatures for streamflow and streamflow source waters, as snow, groundwater and rain, were determined and used to partition source water contributions to streamflow for each watershed. In general, during the 2012 water year, source water contributions to streamflow were as follows: snow 60%, groundwater 20% and rain 20%. The correlations between snow, groundwater and rain contributions to streamflow and MPB killed

area were not statistically significant at $\alpha \leq 0.05$ ($p_{snow} = 0.582$, $p_{groundwater} = 0.543$ and $p_{rain} = 0.897$).

While Colorado has suffered extensive forest kill since the onset of the MPB epidemic, the results of this study suggest that MPB killed watershed area has little to no effect on peak streamflow, date of peak streamflow, annual water yield or streamflow generation mechanisms.

ACKNOWLEDGEMENTS

This project would not have been possible without the support of many people. I would like to offer sincere thanks to my advisor, Dr. John Stednick, whose expertise, support, and patience added considerably to this project and my graduate experience. I would like to acknowledge Dr. Steven Fassnacht and Dr. Michael Ronayne for generously serving as committee members. This project was funded by the Colorado Agricultural Experiment Station at Colorado State University.

I would also like to thanks Dr. Dave Williams and Craig Cook at the University of Wyoming Stable Isotope Facility for guiding me through the field of stable isotope analysis and interpretation. Thank you to those in the Stable Isotope Facility laboratory, including Chandelle MacDonald and Patrick Warden for their help processing my many samples.

Additional thanks go out to Megan Horne and Erin Donnelly whose help collecting samples across the expansive study area was greatly appreciated. Thank you to Austin Seback for his help with the GIS portion of this study. Finally, I would like to thank my family, especially my husband Jake, for their continued support throughout graduate school.

TABLE OF CONTENTS

ABSTRACT ii

ACKNOWLEDGEMENTS iv

LIST OF TABLES vii

LIST OF FIGURES viii

INTRODUCTION
- Mountain Pine Beetle 1
- Data Stationarity 4
- Change-point analysis 5
- Isotopy 6
- Streamflow Source Water Contribution Separation 9
- Hypothesis 11
- Study Objectives 11

METHODOLOGY
- Site Description 12
- Mountain Pine Beetle 16
- Data Stationarity 16
- Change-point Analysis 18
- Isotopy 19
- Streamflow Source Water Contribution Separation 21

RESULTS
- Mountain Pine Beetle 22
- Data Stationarity 25
- Change-point Analysis 25
- Isotopy 29
- Streamflow Source Water Contribution Separation 37

DISCUSSION
- Mountain Pine Beetle 41
- Data Stationarity 42
- Change-point Analysis 42
- Isotopy 43
- Streamflow Source Water Separation 45

CONCLUSION 46

RECOMMENDATIONS 47

LITERATURE CITED 49

APPENDIX..55

LIST OF TABLES

Table 1. Study watersheds by USGS site number, location code, site description and period of record. 14
Table 2. Watershed characteristics representing streamflow gauge latitude, streamflow gauge longitude, county, streamflow gauge HUC, watershed contributing area, mean watershed elevation, mean watershed aspect, mean watershed slope, and drainage basin. 17
Table 3. Sampling date for study watersheds. Starred (*) locations represent the location of precipitation samplers near streamflow gauges. Symbols correspond to sample types collected: ◊ streamflow, Δ snow, + groundwater and ○ rain. 20
Table 4. Annual and cumulative MPB watershed kill area for each study watershed is shown. 24
Table 5. Results of data-stationarity analysis. For $n \geq 10$ a Z-test statistic was used, for $n < 10$ an S-test statistic was used. Watersheds did not exhibit significant trends (no significance, ns) for peak streamflow, date of peak streamflow, or water yield during the period of record. 27
Table 6. Watershed specific mean isotope concentrations for each sample type for October 2011- November 2012. Sample number, δ^2H, $\delta^{18}O$ and *d*-excess are shown. Snow and rain sample types reflect mean isotope concentrations for samples collected over the entire study area. 34
Table 7. Parameters describing statistical strength of relations between mean source contributions to streamflow and beetle-killed area (%). Represented are sample number (n), correlation coefficient (r_s), t-value, degrees of freedom (df), and p-value. 40

LIST OF FIGURES

Figure 1.Watersheds selected for study based on streamflow records, site access, and beetle activity. 13
Figure 2. Represented are annual minimum, maximum and average (a) precipitation and (b) snow water equivalent (SWE) for the study area derived from SNOTEL. Also shown is the mean annual average for precipitation and SWE. 15
Figure 3. Cumulative (1997-2011) MPB watershed kill area is shown. Watershed areas represented in gray while increasing beetle-killed area (%) is illustrated by a deepening shade of red. 23
Figure 4. Distribution of data for (a) peak streamflow, (b) date of peak streamflow and (c) annual water yield, as well as the Sen's slope estimate for watershed Willow Creek above Willow Creek Reservoir (WCR). Slope estimates were not statistically significant at $\alpha \leq 0.05$. 26
Figure 5. Distribution of residual values (data-mean) for (a) peak streamflow, (b) date of peak streamflow and (c) annual water yield around the mean (μ) for watershed WCR. 28
Figure 6. Rocky Mountain Meteoric Water Line, Global Meteoric Water Line and Local Meteoric Water Line are shown. 30
Figure 7. Isotopic composition of streamflow, snow, groundwater and rain samples acquired from all sites. The LMWL and evaporation lines (r^2=0.765) are shown. 30
Figure 8. Isotopic composition of precipitation from all sites by sampling date shows little effect on spatial distribution; however seasonal effects in isotopic composition of precipitation samples can be seen. 31
Figure 9. Temporal distribution of streamflow samples. 33
Figure 10. *d*-excess values of streamflow, snow, groundwater and rain samples versus sample date are shown to illustrate increased evaporative effect on groundwater samples. 36
Figure 11. (a)Mean, (b) minimum and (c) maximum estimated snow, groundwater and rain source water contributions to streamflow (fraction), as determined from IsoSource. 39

INTRODUCTION

Colorado's high elevation watersheds serve as important water sources. Due to the nature of these watersheds, minor changes in climate can have major effects on ecological functions and hydrologic cycles (Williams et al. 1996). As a result of warming temperatures, compounded with other factors like drought (Carroll et al. 2004) and increased forest density (Fettig et al. 2007), mountain pine beetle (*Dendroctonus ponderosae* Hopkins) (MPB) populations in the Rocky Mountain region were at epidemic conditions (Man 2012). Altered watershed dynamics as a result of MPB caused tree mortality may cause changes in hydrologic processes, potentially altering streamflow generation mechanisms and streamflow. As Colorado experiences increasing demand on water supplies (Colorado Water Conservation Board 2010), identifying relations between declining forested watershed health and water resources is of importance.

Mountain Pine Beetle

Since the onset of the beetle epidemic in the mid 1990's, MPB has been the primary cause of tree mortality in Colorado forests (CSFS 2011). The present outbreak which began in 1996, has predominantly affected lodgepole pine (*Pinus contorta*) forests, however other coniferous tree species including limber (*Pinus flexilis*) and ponderosa pine (*Pinus ponderosa*) have also suffered insect damage (CSFS 2011). Forest damage in Colorado has continued, with an additional 125 km^2 of forest being damaged in 2012 alone and a total of 13700 km^2 of forest killed since the beginning of the epidemic (USDA Forest Service 2012). A decrease in the annual area damaged was observed in 2011 and 2012, and is attributed to the lack of suitable host trees (USDA Forest Service 2012).

Pine tree death due to MPB invasion takes on three distinct phases; green, red and gray (Wulder et al. 2006). The one year regeneration cycle of a MPB occurs during the green tree phase, while the red and gray tree phases occur post-attack (Wulder et al. 2006). The MPB life cycle itself, is comprised of four stages; egg, larva, pupa and adult (Safranyik and Carroll 2006). In late summer, once a suitable living green host tree has been selected, adult beetles bore into the tree and create egg galleries under the tree bark (Safranyik 1989; Safranyik and Carroll 2006). It is in the galleries that adults mate and females lay their eggs (Safranyik 1989; Safranyik and Carroll 2006). Mountain pine beetles transmit blue stain fungus (*Grosmannia clavigera*) to host trees during construction of egg galleries (Sanfranyik and Carroll 2006). The fungus prohibits the tree from transpiring, blocking resin production and lowering the tree's defenses against the beetle attack (Hubbard et al. 2013). As winter ends, the larvae tunnel away from the gallery and feed on the beetle-transmitted blue-stain fungus infected phloem through the spring (Safranyik and Carroll 2006). During June and July larvae develop into pupae and fully matured adults leave the host tree in late July to seek a new host in which to lay their eggs, thus completing the one year cycle (Safranyik 1989; Safranyik and Carroll 2006).

The first year after attack the needles on an infected tree will fade from green to red and the needles will begin to drop (Wulder et al. 2006). The gray phase occurs approximately three years after the initial attack when the host tree has lost all its needles (British Columbia Ministry of Forests 1995).

The similarity in forest hydrological processes under MPB attack, and death and tree removal due to timber harvesting lead many to compare changes in the hydrologic cycle due to stand death from MPB infestation to changes in the hydrologic cycle caused by timber harvesting (MacDonald and Stednick 2003; Hélie et al. 2005; Boon 2007; Boon 2008). Absence of the forest canopy cover either by harvesting or needle loss decreases interception and evapotranspiration (ET), thus decreasing soil moisture depletion (Troendle and Leaf 1981). As less water is needed for soil moisture recharge, once snowmelt begins, the excess meltwater enters the stream (Troendle and Leaf 1981). The excess meltwater will alter relative contributions to streamflow from source waters; thereby changing streamflow generation mechanism in MPB affected forests.

Additionally, decreased canopy cover and consequently decreased snowfall interception, will allow increased snow accumulation on the forest floor and increased peak snow water equivalent (SWE) (Troendle and King 1985; Troendle 1987; Troendle and Reuss 1997; Winkler et al. 2005). Incoming short wave radiation transmission to the forest floor will increase due to decreased canopy cover (Winkler et al. 2005; Boon 2008), potentially affecting snowmelt rates. The onset of snowmelt will likely advance in time as more radiation reaches the snow pack. The rate of melt will increase with increased radiation.

As a result of decreased canopy cover and interception, timber harvesting has been shown to increase annual water yield, and some peak flows (Stednick 1996). Beetle-killed watersheds, like clearcut watersheds, have been shown to have increased annual water yields and increased peak flows (Love 1955; Bethlahmy 1974; Bethlahmy 1975; Potts 1984).

Greater canopy loss in gray phase stands versus red phase stands may result in increased water yield and higher and advanced (earlier) peak flows within the watershed. Precipitation interception and SWE in red phase stands will not differ significantly from live stands because the affected trees still retain a large percentage of their needles (Pugh and Small 2011). The degree of canopy loss in red phase stands generates negligible net increases to soil water and has little effect on other components of the hydrograph (Pugh and Small 2011). Hydrologic processes in gray phase stands should shift more toward those observed in clearcuts. As canopy cover decreases, SWE will increase, as will short wave radiation transmission (Pugh and Small 2011). Greater short wave radiation transmission to an increased snowpack, in combination with a decrease in ET within gray phase MPB affected stands, may cause snowmelt to be a larger contributor to soil water in gray phase stands than in green or red phase stands (Pugh and Small 2011). Gray phase stands will also experience decreased longwave radiation absorption and reemission (Rouse 1984) which may contribute to changes in hydrologic cycling within the watershed. Given the time elapsed since the onset of the MPB infestation, a large portion of affected forests will be in the gray phase.

This study will determine the effects of MPB caused tree mortality on streamflow and streamflow generation mechanisms. Multiple approaches will be used. First, streamflow records from forested watersheds will be assessed to determine if any streamflow changes are the result of climate variability. Streamflow records will be tested for stationarity, which means that no significant changes in the statistical properties of a time series occur. Streamflow records including peak flow, date of peak flow and annual water yield will be assessed for trends and change-points in the records. For this study, water yield is defined as amount of runoff from a watershed. A change-point in streamflow records will be correlated to a change-point in MPB caused forest mortality. Isotopic signatures of streamflow will be used in a mixing model for hydrograph separation of precipitation and groundwater components. A brief review of these subject areas follows.

Data Stationarity

Stationarity is when statistical properties of a time series do not change with time (Rao et al. 2003). Historically, hydrologic modeling has been based on the principle of stationarity; it was believed that the statistical properties of hydrologic events, like the frequency of floods, were unchanging with time (Milly et al. 2008). In light of climate variability, the principle of stationarity in hydrological processes has been revisited.

The Mann-Kendall trend test is commonly applied to hydrologic time series data to identify the presence, direction and magnitude of trends. This is a robust, non-parametric test used to detect monotonic trends based on rank, making the test less sensitive to outliers or missing data (Gilbert 1987, Rao et al. 2003). In monotonic trends, statistical parameters, like mean and median, may change over time in one direction, but not necessarily continuously or linearly (Rao et al. 2003). Recent applications of the Mann-Kendall trend test include the effects of land use changes and climate change on streamflow (Zhang et al. 2008; Salarijazi et al. 2012). Trend tests are frequently applied to hydrologic data in conjunction with change-point analysis to identify the point at which abrupt changes in the time series occur due to land use changes or climate variability (Ma et al. 2008; Zhang et al. 2008; Salarijazi et al. 2012). If a trend is detected, a change-point analysis helps identify that point in time.

Change-point Analysis

Change-point analysis is conducted with a non-parametric test for homogeneity. The Pettitt test was developed to identify change-points in hydrologic time series when the exact time of change is unknown (Pettitt 1979). This approach determines significant changes in mean values of a series, pinpointing abrupt changes in the record. The test counts the number of times a member of the first sample exceeds a member of the second sample. If a change point is detected, the time series is divided into two parts around the timing of the change point. The Pettitt test is frequently used in combination with statistical trend tests to assess the effects of watershed changes on hydrologic time series data (Ma et al. 2008; Zhang et al. 2008; Salarijazi et al. 2012). A change-point can distinguish streamflow changes due to natural disturbance or land use changes from streamflow changes due to climate variability. In the case of this study, a change-point in annual peak flow, date of peak flow and annual water yield data correlating with MPB caused watershed mortality would identify streamflow changes due to MPB activity.

Decreased forest health due to MPB infestation has the potential to change hydrologic processes. As previously mentioned, as forest mortality progresses from the red to gray phase, forest canopy loss will increase and interception will decrease. Increased snowpack coupled with increased radiation results in increased snowmelt water to groundwater and hence streamflow. Using natural stable isotope analysis of the hydrologic cycle in a mixing model can be used to determine contributions of precipitation and groundwater to streamflow.

Isotopy

Stable isotopes have become a popular tool to illustrate the specifics of, and changes in, the hydrologic cycle, particularly streamflow generation mechanisms. Several species of the water molecule exist naturally in various abundances (Singh and Kumar 2005). ^{2}H (deuterium) and ^{18}O are two isotopes that are frequently used as hydrologic tracers. These isotopes are relatively unreactive with basin materials, and source waters (i.e. rain, snow and groundwater) possess different isotopic compositions due to isotopic fractionation (Kendall and Caldwell 1998).

Phase changes of a water molecule cause mass-dependent isotopic fractionation of hydrogen and oxygen (Kendall and Caldwell 1998). Fractionation implies that different phases of water possess unique isotopic abundances, representing differing ratios of heavy (^{2}H and ^{18}O) to light (^{1}H and ^{16}O) isotopes (Kendall and Caldwell 1998). Two types of fractionation can occur; equilibrium fractionation and kinetic fractionation.

Rayleigh equations, generally presented as equilibrium fractionation, are characterized by a series of equations dictating the partitioning of isotopes between two reservoirs in equilibrium (Kendall and Caldwell 1998). The Rayleigh process can be used to describe isotope separation during evaporation and condensation processes at 100% humidity (Kendall and Caldwell 1998). Due to differences in mass, the fractionation associated with evaporation of liquid water to form water vapor causes lighter isotopes to react first, leaving the residual liquid water enriched in heavy isotopes (Kendall and Caldwell 1998). The opposite is true for condensation of water vapor. Heavy isotopes in water vapor will condense first, causing precipitation to be enriched in heavy isotopes relative to the parent cloud (Kendall and Caldwell 1998).

Kinetic fractionation, unlike equilibrium fractionation, is unidirectional, leaving the product of the process isolated from the reactant (Kendall and Caldwell 1998). The Global Meteoric Water Line (GMWL) is the result of both equilibrium and kinetic fractionation (Ingraham 1998). During this process, ocean water is evaporated under kinetic fractionation and subsequent condensation of global precipitation occurs via equilibrium fractionation (Ingraham 1998). As oceanic water vapor moves inland and rainout from clouds occurs, the water vapor becomes progressively depleted of heavy isotopes with each precipitation event, known as the continental effect (Dansgaard 1964; Dawson and Simonin 2011). Depletion of heavy isotopes also occurs as the result of a latitude or temperature effect whereby water condensing at cooler temperatures is increasingly depleted of heavy isotopes (Dansgaard 1964). The combination of traveling and condensing water vapor creates varying isotopic signatures for precipitation at different continental locations. The resultant GMWL yields a linear relation representing concentrations of ^{2}H and ^{18}O in global precipitation that can be described with the following equation (Kendall and Caldwell 1998):

$$\delta^2H = 8 * \delta^{18}O + 10 \quad (1)$$

A Local Meteoric Water Line (LMWL) can also be developed based on local meteorology. A LMWL should yield a somewhat different slope and intercept when compared to the GMWL (Ingraham 1998).

The intercept of + 10 (‰) in the GMWL represents the *deuterium*-excess (*d*-excess) and can be defined by the following equation (Dansgarrd 1964).

$$d - excess = \delta^2H - 8 * \delta^{18}O \quad (2)$$

This *d*-excess parameter is indicative of the process of kinetic fractionation that is associated with evaporation of surface water, at a relative humidity less than 100% (Dansgaard 1964; Dawson and Simonin 2011). As water undergoes evaporation, the residual liquid water will become enriched in ^{18}O more than ^{2}H, this enrichment causes the *d*-excess to decrease in the residual water (Gupta 2010). Changes in the *d*-excess parameter will show samples that experience evaporation plotted below the GMWL (Gupta 2010).

Precipitation as snow will experience depletion of heavy isotopes and slightly decreased *d*-excess values when compared to precipitation as rain (Gat 2010). Higher *d*-excess values are observed in snow, and attributed to kinetic fractionation due to water vapor deposition during formation (Jouzel and Merlivat 1984). Solid precipitation will essentially hold an isotopic signature during formation until surface processes begin after accumulation on the land surface (Gat 2010). Once accumulated snow begins to melt, water containing light isotopes will melt out first, causing the snowpack to become more enriched in heavy isotopes as melt continues (Cooper 1998). Because the snowpack becomes more enriched in heavy isotopes, the isotopic signature of meltwater will increase over time (Cooper 1998). The isotopic composition of the meltwater should be higher than that of the original snowpack due to sublimation from the snowpack (Rodhe 1998). Meltwater in snow dominated systems has been seen to be substantially more depleted in stable isotopes than mean annual precipitation and groundwater creating an ideal hydrologic tracer (Rodhe 1998).

Soilwater or meltwater that is in contact with the atmosphere will experience evaporation and exchange with atmospheric water vapor which will cause enrichment of heavy isotopes (Cooper 1998). The effects of evaporation on soil water are depth dependent, as evaporation effects decrease with increasing soil depth (Gat 2010). Because evaporative effects decrease with depth, in the absence of ground water samples, groundwater can be extracted as a surrogate.

These environmental tracers can be used to identify streamflow generation mechanisms in MPB affected watersheds by partitioning contributions to streamflow between precipitation and groundwater. A relation between increased groundwater contributions to streamflow from watersheds with increased area of MPB caused forest mortality would be expected due to changes in forest health.

Streamflow Source Water Separation

Streamflow source water separation involves partitioning streamflow between multiple source components and can be accomplished through analytical or graphical methods. Analytical separation methods utilize differences in the isotopic composition of source waters to partition streamflow between multiple sources. Two-component models are used to quantify groundwater and direct runoff contributions to streamflow and multi-component models can quantify contributions from multiple sources. IsoSource is a computer program that utilizes the multi-component mass balance equation to create a stable isotope mixing model to partition streamflow among two or more sources (Phillips and Gregg 2003).

Declining forest health has the potential to alter hydrologic processes. Efforts to quantify changes in water yield as a result of the MPB epidemic have been made (Love 1955; Bethlahmy 1974; Bethlahmy 1975; Potts 1984; Hèlie et al. 2005; Boon 2008); however differences in streamflow generation mechanisms as proposed here may better identify the effects on water yield. This study will determine changes in groundwater contributions to streamflow in watersheds with varying degrees of MPB caused tree mortality through environmental isotope tracers and hydrograph separation methods. As the beetle-killed area increases, greater groundwater contributions to streamflow would be expected.

HYPOTHESIS

Mountain pine beetle caused tree mortality changes streamflow generation mechanisms and streamflow as measured by annual water yield, peak flow and date of peak flow and contribution of groundwater to streamflow will increase with increased beetle-killed watershed area.

STUDY OBJECTIVES

To determine if beetle-killed forest watersheds have detectable changes in annual water yield, peak flows or groundwater contribution to streamflow, the following objectives were conducted:

1) Determine MPB caused tree mortality for hydrologic unit (HUC) level 8 watersheds in north-central Colorado.
2) Test data stationarity of long-term annual water yield, peak flows and date of peak flow using the Mann-Kendall test and the Pettit change-point test.
3) Determine isotopic signatures of precipitation (as snow and rain), soil moisture (surrogate for groundwater) to determine each contribution to streamflow as a function of beetle-killed area.

METHODOLOGY

Site Description

The study area is located in north central Colorado (Figure 1) to complement ongoing study efforts. The forested watersheds are largely federal lands with little land use change over time. The landscape within the study area consists of mountainous subalpine mixed conifer forest, including lodgepole pine (*Pinus contorta*), ponderosa pine (*Pinus ponderosa*), limber pine (*Pinus flexilis*), Douglas-fir (*Pseudotsuga menziesii*), white fir (*Abies concolor*), subalpine fir (*Abies lasiocarpa*), spruce (*Picea pungens*) and Rocky Mountain juniper (*Juniperus scopulorum*) (CSFS 2011). Study area hydrology is snowmelt dominated, exhibiting peak flows in the spring with little streamflow response to summer precipitation events.

Within the study area, 21 watersheds were selected (Figure 1). The watersheds were selected based on the availability of continuous, long-term streamflow records (Table 1), being on largely federal lands with little to no land use change, and site access. This study was conducted largely over the 2012 water year with sampling extending from Oct 2011 through Nov 2012. Precipitation and SWE derived from SNOTEL (http://www.wcc.nrcs.usda.gov/snow/) data over the study area was below average during this time frame (Figure 2).

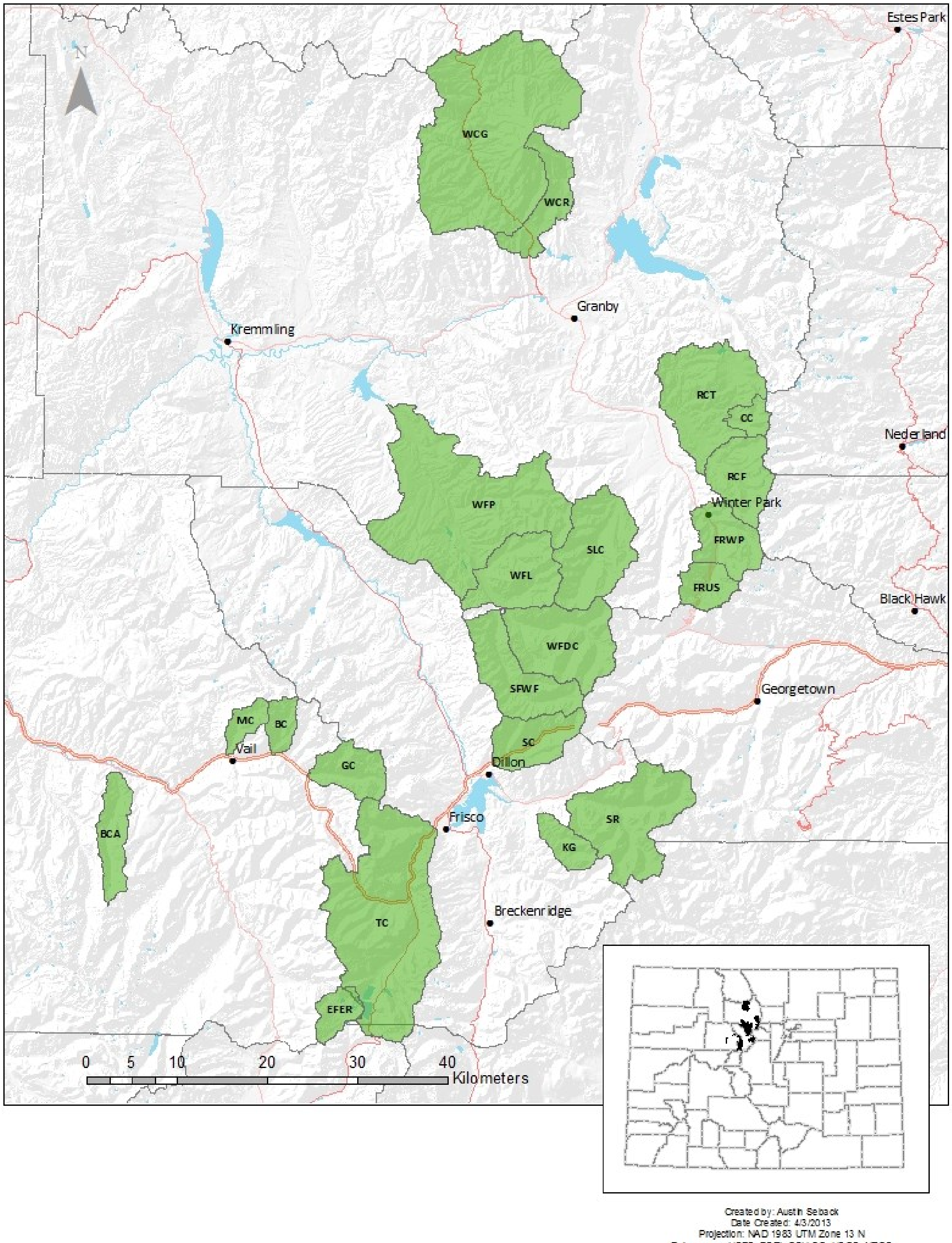

Figure 1.Watersheds selected for study based on streamflow records, site access, and beetle activity.

Table 1. Study watersheds by USGS site number, location code, site description and period of record.

USGS Site Number	Location	Description	Period of Record
9061600	EFER	East Fork Eagle River nr Climax, CO	2003-2012
9047500	SR	Snake River nr Montezuma, CO	1990-2012
9050100	TC	Tenmile Crk blw N. Tenmile Crk at Frisco, CO	1990-2012
9035700	WFDC	Williams Fork abv Darling Crk nr Leal, CO	1990-2012
9022000	FRUS	Fraser River at Upper Sta. nr Winter Park, CO	1990-2012
9065500	GC	Gore Crk at Upper Sta. nr Minturn, CO	1990-2012
9066200	BC	Booth Crk near Minturn, CO	1990-2012
9036000	WFL	Williams Fork nr Leal, CO	1990-2012
9024000	FRWP	Fraser River at Winter Park, CO	1990-2012
9037500	WFP	Williams Fork nr Parshall, CO	1990-2012
9035900	SFWF	South Fork of Williams Fork nr Leal, CO	1990-2012
9032100	CC	Cabin Crk nr Fraser, CO	1990-2012
9047700	KG	Keystone Gulch nr Dillon, CO	1990-2012
9067000	BCA	Beaver Crk at Avon, CO	1990-2012
9051050	SC	Straight Crk blw Laskey Gulch nr Dillon, CO	1990-2012
9032000	RCF	Ranch Crk nr Fraser, CO	1990-2012
9026500	SLC	St. Louis Crk nr Fraser, CO	1990-2012
9033100	RCT	Ranch Crk blw Meadow Crk nr Tabernash, CO	1998-2005
9066300	MC	Middle Crk nr Minturn, CO	1990-2012
9020500	WCR	Willow Crk abv Willow Crk Reservoir, CO	1990-2012
9020000	WCG	Willow Crk nr Granby, CO	1936-1953

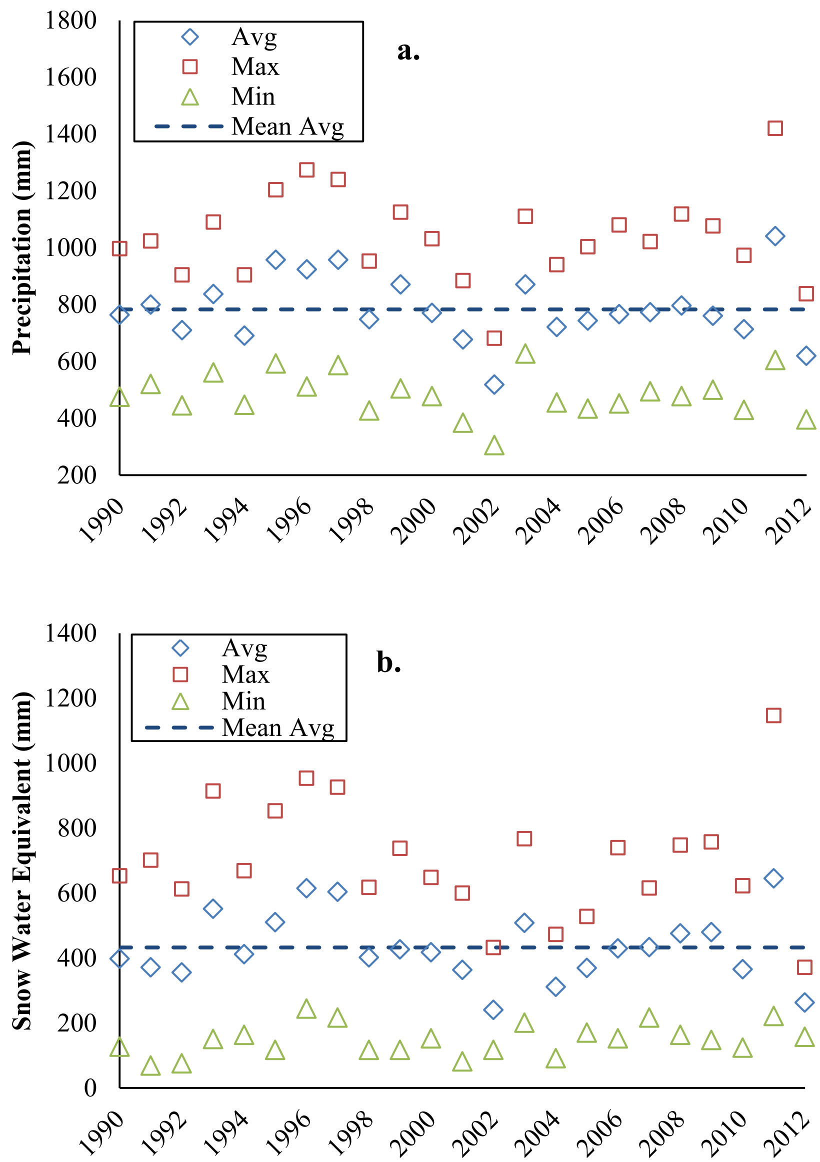

Figure 2. Represented are annual minimum, maximum and average (a) precipitation and (b) snow water equivalent (SWE) for the study area derived from SNOTEL. Also shown is the mean annual average for precipitation and SWE.

Mountain Pine Beetle

Area and percent of watershed area killed by MPB were quantified using a geographic information system (GIS). Coniferous forested layer was based on National Land Cover Data (http://landcover.usgs.gov/classes.php) while MPB kill layer was derived from the United State Forest Service Aerial Detection Surveys (http://www.fs.usda.gov/detail/r2/forest-grasslandhealth/?cid=fsbdev3_041629). All MPB related characteristics reflect cumulative damage between 1997 and 2011 (Table 2).

Data Stationarity

Streamflow records of daily streamflow, instantaneous annual peak flow and peak flow date were accessed through the USGS National Water Information System (NWIS), and were acquired for 20 of the 21 gauges. Streamflow records for Willow Creek above Willow Creek Reservoir, CO were acquired from the Northern Colorado Water Conservancy District. Due to seasonal operation, approximation of daily streamflow values via linear interpolation between missing values was carried out for three sites: Willow Creek above Willow Creek Reservoir, CO, Ranch Creek below Meadow Creek near Tabernash, CO and Snake River near Montezuma, CO. The site, Willow Creek near Granby,CO was excluded from data stationarity analysis due to the lack of long-term streamflow records in the past two decades. Daily streamflow records were used to calculate annual water yield. Annual water yield, annual peak flow and date of peak flow were analyzed for stationarity using MAKESENS (Salmi et al. 2002), an Excel based application of the Mann-Kendall test for data stationarity.

Table 2. Watershed characteristics representing streamflow gauge latitude, streamflow gauge longitude, county, streamflow gauge HUC, watershed contributing area, mean watershed elevation, mean watershed aspect, mean watershed slope, and drainage basin.

Location	Latitude	Longitude	County	HUC	Area (km^2)	Mean Elevation (meter)	Mean Aspect (direction)	Mean Slope (%)
WCP	40° 20' 59.100"	106° 05' 24.730"	Grand	14010001	n/a	2940	n/a	n/a
EFER	39° 24' 30.237"	106° 14' 57.015"	Eagle	14010003	21	3470	SE	26
SR	39° 36' 13.204"	105° 56' 32.983"	Summit	14010002	108	3517	S	41
TC	39° 34' 24.210"	106° 06' 35.983"	Summit	14010002	237	3343	S	34
WFDC	39° 47' 43.112"	106° 01' 32.302"	Grand	14010001	167	3386	S	40
FRUS	39° 50' 38.203"	105° 45' 04.981"	Grand	14010001	26	3498	S	39
GC	39° 37' 26.209"	106° 16' 38.976	Eagle	14010003	37	3379	S	47
BC	39° 38' 47.204"	106° 19' 20.993"	Eagle	14010003	17	3264	S	48
WFL	39° 49' 55.187"	106° 03' 20.998"	Grand	14010001	304	3160	S	34
FRWP	39° 53' 53.203"	105° 46' 33.985"	Grand	14010001	72	3273	S	36
WFP	39° 59' 53.992"	106° 10' 49.299"	Grand	14010001	539	2891	S	26
SFWF	39° 47' 48.720"	106° 01' 49.970"	Grand	14010001	72	3351	S	40
CC	39° 59' 02.182"	105° 44' 40.010"	Grand	14010001	14	3273	SW	35
KG	39° 35' 33.211"	105° 58' 19.015"	Summit	14010002	23	3341	S	35
BCA	39° 37' 40.210"	106° 31' 20.000"	Eagle	14010003	38	3157	S	36
SC	39° 38' 16.201"	106° 02' 22.983"	Summit	14010002	48	3419	S	36
RCF	39° 56' 53.192"	105° 45' 54.003"	Grand	14010001	51	3166	SW	30
SLC	39° 54' 29.191"	105° 52' 40.012"	Grand	14010001	85	3309	S	35
RCT	39° 59' 56.993"	105° 49' 37.083"	Grand	14010001	156	2961	SW	25
MC	39° 38' 45.016"	106° 22' 54.006"	Eagle	14010001	16	3148	SW	36
WCR	40° 09' 13.191"	105° 58' 47.983"	Grand	14010001	329	2846	S	28
WCG	40° 10' 43.185"	106° 00' 31.013"	Grand	14010001	285	2958	S	29

The null hypothesis of no trend is tested against an alternative hypothesis of a trend present at a given confidence interval (Gilbert 1987). Two test parameters are generated: a test statistic which signifies the significance of the trend, and a Sen's slope estimate that reflects the direction and rate of change of the trend (Gilbert 1987). When fewer than 10 data values are evaluated an *S*-statistic is generated and a *Z*-statistic is generated for 10 or more data values. Under the null hypothesis of no trend, the test statistic will be zero. A positive test statistic means values taken later in time are greater than values taken earlier indicative of an upward trend, and the opposite is true for a negative test statistic, indicative of a downward trend. To assess the significance of the trend, the absolute value of the test statistic or corresponding probability value, depending on the number of data values being considered, is compared against a significance level, alpha (α) (Gilbert 1987). If statistically significant trends in peak flow, date of peak flow or annual water yield were detected, a change-point analysis was conducted.

Change-point analysis

A non-parametric change-point test (Pettit 1979) was carried out on long-term streamflow records of annual water yield, annual peak flow, and date of peak flow. A test statistic counts the number of time a member of the first sample exceeds a member of the second sample. Its statistic and associated probability are used to assess the significance of the change-point in the distribution.

Cumulative sum analysis of peak streamflow, peak streamflow timing, annual water yield and annual MPB watershed kill area versus time was used to graphically identify changes in streamflow records with increasing MPB watershed area mortality.

Isotopy

Samples of streamflow at the streamflow gauges were collected in 20mL polypropylene scintillation bottles on multiple dates (Table 3). Sample bottles were capped while immersed in the sample water *in-situ* to ensure no head space.

Precipitation samplers were modified from International Atomic Energy Agency precipitation sampler design (IAEA 1997). The samplers consist of a brown one liter polypropylene sample bottles with the top cut off and a small amount (< 2cm) of light paraffin oil added, allowing the light paraffin oil to sit on top of the liquid precipitation, preventing evaporation and isotopic enrichment between sampling events. The sample bottles sat roughly one meter above the soil surface to allow for increasing snow depth through the season. Depth-integrated snow samples through depth of snowpack were taken at all sites when snow was present for sampling.

Soil water samples were used as a surrogate for groundwater samples (Gat 2010). Surface soil samples (< 30cm) were taken on two sampling trips (Table 3). Soil moisture extraction and isotopic analysis was conducted at the University of Wyoming Stable Isotope Facility (Laramie, WY).

Soil water was extracted using a water line extraction system at the University of Wyoming Stable Isotope Facility (UWYSIF 2012). The samples were analyzed for $\delta^{18}O$ and $\delta^{2}H$, expressed as parts per thousand (‰) relative to Vienna Standard Mean Ocean Water (VSMOW). Samples were analyzed using the Los Gatos LWIA Wavelength-Scanned Cavity Ring Down Spectrometer (UWYSIF 2012).

Table 3. Sampling date for study watersheds. Starred (*) locations represent the location of precipitation samplers near streamflow gauges. Symbols correspond to sample types collected: ◊ streamflow, Δ snow, + groundwater and ○ rain.

Location	**8-Oct 2011**	**12-Nov 2011**	**21-Jan 2012**	**30-Mar 2012**	**27-Apr 2012**	**14-May 2012**	**15-Jun 2012**	**10-Jul 2012**	**17-Aug 2012**	**3-Nov 2012**
WCP*			Δ	Δ +	+		○	○	○	○
EFER*				◊ Δ +	◊ +	◊	◊ ○		◊ ○	◊ ○
SR		◊	◊ Δ	◊ Δ	◊ +	◊	◊	◊	◊	◊
TC		◊	◊ Δ	◊ Δ +	◊ +	◊	◊	◊	◊	◊
WFDC	◊	◊		◊ Δ	◊ +	◊	◊	◊	◊	◊
FRUS*	◊				◊ Δ +	◊ ○	◊ ○	◊ ○	◊ ○	◊ ○
GC*				◊ +	◊ Δ +	◊ ○	◊ ○	◊ ○	◊ ○	◊ ○
BC				◊ +	◊ +	◊	◊	◊	◊	◊
WFL	◊			◊ Δ +	◊ +	◊	◊	◊	◊	◊
FRWP				◊ Δ +	◊ +	◊	◊	◊	◊	◊
WFP		◊	◊	◊ +	◊ +	◊	◊	◊	◊	◊
SFWF*	◊	◊	◊ Δ	◊ Δ +	◊ +	◊ ○	◊ ○	◊ ○	◊ ○	◊ ○
CC*	◊	◊		◊ Δ +	◊ Δ +	◊ ○	◊ ○	◊ ○	◊ ○	◊ ○
KG*		◊	◊ Δ	◊ Δ +	◊ +	◊ ○	◊ ○	◊ ○	◊ ○	○
BCA				◊ +	◊ +	◊	◊	◊	◊	◊
SC*		◊	◊ Δ	◊ +	◊ +	◊ ○	◊ ○	◊ ○	◊ ○	◊ ○
RCF	◊			◊ Δ +	◊ +	◊	◊	◊	◊	◊
SLC*	◊	◊	Δ	◊ Δ +	◊ +	◊ ○	◊ ○	◊ ○	◊ ○	◊ ○
RCT	◊			◊ Δ +	◊ +	◊	◊	◊	◊	◊
MC				◊ +	◊ +	◊	◊	◊	◊	◊
WCR		◊	◊ Δ	◊ +	◊ +	◊	◊	◊	◊	◊
WCG	◊	◊	Δ	◊ +	◊ +	◊	◊	◊	◊	◊

Streamflow Source Water Separation

Using the isotope values from the samples collected over the 2012 water year, isotope signatures of ^{2}H versus ^{18}O for streamflow, snow, soil water and rain were plotted. Differences in these signatures allowed for the use of hydrograph separation techniques to partition annual contributions of precipitation and groundwater to streamflow.

IsoSource (Phillips and Gregg 2003) was used to partition streamflow among snow, rain and groundwater contributions using ^{2}H and ^{18}O annual isotopic signatures. IsoSource expands upon the 2-component mass balance equations to allow for *n*+1 sources. The following governing equations are employed to generate a multi-source mixing analysis:

$$\delta_M = f_A\delta_A + f_B\delta_B + f_C\delta_C \tag{3}$$

$$1 = f_A + f_B + f_C \tag{4}$$

where *M* is the mixture, or streamflow, *A*, *B* and *C* are the sources, δ is the annual isotopic signature and *f* is the fraction of the mixture. This yields a mathematically underdetermined system of two equations and three unknowns, which does not allow for a unique solution. Instead, combinations of feasible source contributions are analyzed based on an increment value (1%). Combinations are considered feasible if the sum of those source mixtures are within a tolerance value. The tolerance value is calculated as half the increment value times the maximum difference between sources:

$$tolerance\ value = \frac{1}{2}\begin{pmatrix} increment \\ value \end{pmatrix} \times \begin{pmatrix} \max source\ isotopic\ concentration\ (‰) - \\ \min isotopic\ concentration\ (‰) \end{pmatrix} \tag{5}$$

After analysis, all feasible source proportion combinations are output as well as the distribution of these combinations, including, for example, the minimum and maximum proportions, representing the range of the components' feasible contributions to the mixture. (Phillips and Gregg 2003)

RESULTS

Mountain Pine Beetle

Annual MPB-killed watershed area was used to calculate cumulative beetle-killed area for each watershed between 1997 and 2011 (Table 4). Watershed characteristics, including watershed area, were originally determined for sub-basins. Water chemistry and streamflow generation mechanisms are reflective of all upstream activities. In order to relate water chemistry and streamflow generation mechanisms with the appropriate basin, major basin characteristics were determined from their contributing sub-basins. Cumulative beetle-killed area between 1997 and 2011 ranged from 5 to 82% of the watershed area (Table 4). The map (Figure 3) represents beetle kill in stand-alone major basins and sub-basins.

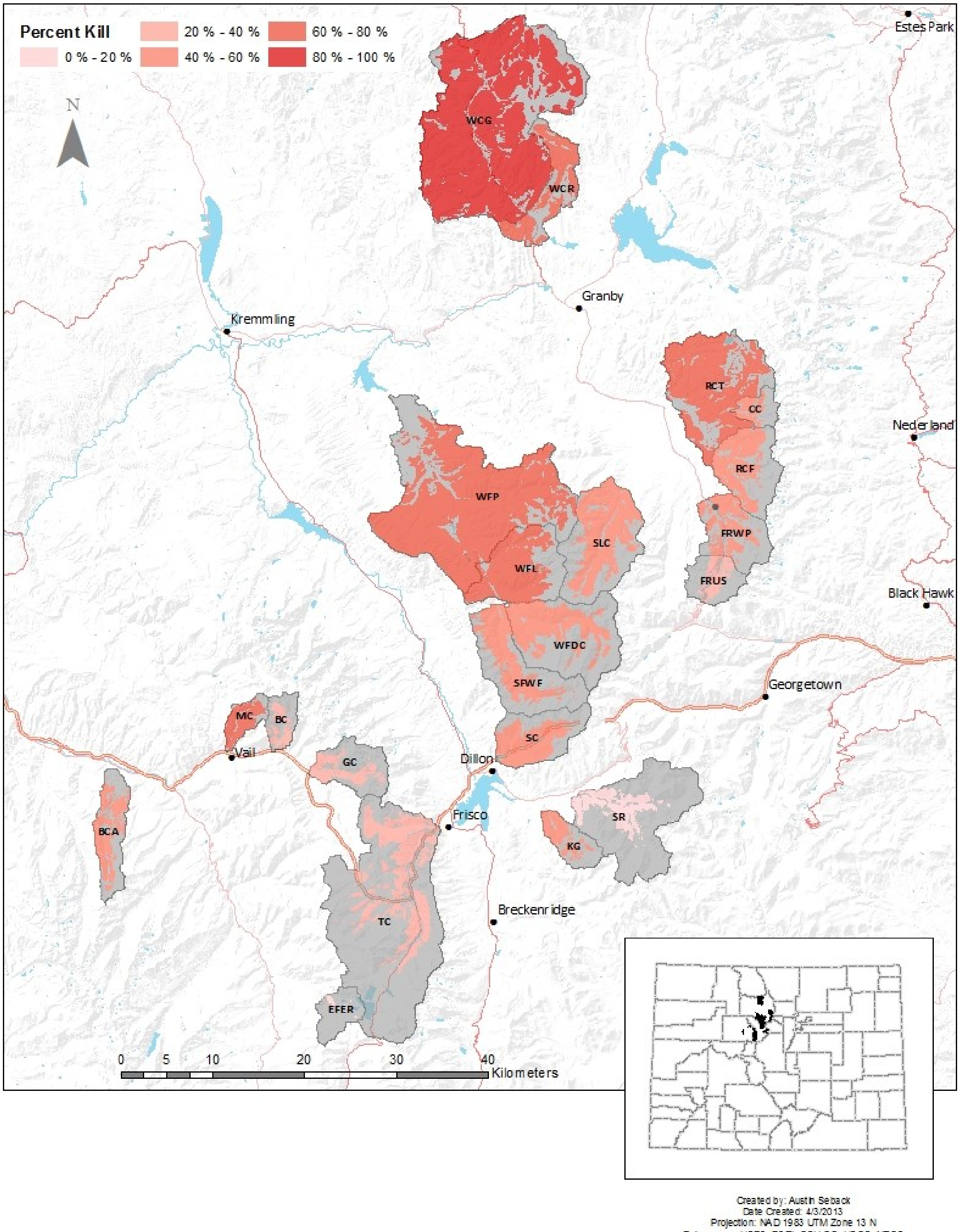

Figure 3. Cumulative (1997-2011) MPB watershed kill area is shown. Watershed areas represented in gray while increasing beetle-killed area (%) is illustrated by a deepening shade of red.

Table 4. Annual and cumulative MPB watershed kill area for each study watershed is shown.

		Cumulative Beetle-Killed Area (%)															
Location	**Watershed Area (km^2)**	**1997**	**1998**	**1999**	**2000**	**2001**	**2002**	**2003**	**2004**	**2005**	**2006**	**2007**	**2008**	**2009**	**2010**	**2011**	**Cumulative Beetle-Killed Area (km^2)**
EFER	21.3	0.00	0.061	0.061	2.7	3.1	3.3	3.5	3.7	3.9	4.0	4.4	4.4	4.4	4.9	5.1	1.09
SR	108	1.0	3.2	3.5	4.3	5.0	5.4	6.4	10	11	12	14	15	18	19	19	20.9
TC	237	0.23	2.9	3.5	4.8	4.9	6.0	6.5	8.7	9.9	11	13	18	20	22	23	54.2
WFDC	167	0.54	0.88	1.2	1.5	1.6	2.3	5.8	15	17	18	19	20	20	23	23	39.0
FRUS	26.3	1.2	1.3	1.8	4.8	7.2	9.3	10	16	19	23	25	28	30	32	32	8.39
GC	37.2	2.9	7.4	9.0	10	13	14	18	23	25	26	27	30	32	32	33	12.1
BC	17.3	6.6	8.2	9.7	14	17	23	25	30	31	33	34	36	37	38	38	6.57
WFL	304	1.0	2.5	3.5	4.3	4.7	8.5	15	28	31	33	34	36	37	39	39	118
FRWP	71.6	0.63	3.0	3.5	4.9	6.4	7.6	8.2	12	15	20	30	34	38	39	40	28.3
WFP	539	0.71	3.7	5.8	7.5	9.8	19	26	36	39	41	41	42	42	43	43	232
SFWF	71.5	0.88	2.9	5.1	6.3	7.4	10	17	28	33	36	39	40	43	44	44	31.5
CC	14.3	0.00	2.7	2.7	4.5	6.0	6.0	6.0	6.5	8.3	23	32	37	42	46	47	6.77
KG	23.1	0.00	0.44	1.1	1.8	1.8	1.9	2.1	5.8	12	14	18	35	46	48	48	11.2
BCA	38.1	1.8	6.4	7.8	11	14	16	16	22	24	38	39	41	43	48	49	18.6
SC	47.8	4.4	4.6	4.6	4.8	4.9	6.3	9.1	28	38	42	50	52	54	54	54	25.9
RCF	51.3	0.22	3.2	3.3	3.7	4.4	5.4	8.0	13	19	29	46	50	53	55	55	28.5
SLC	85.1	4.4	10	11	14	15	15	23	30	40	47	52	55	56	59	59	50.6
RCT	156	0.26	2.7	2.9	3.1	3.9	5.2	8.0	14	29	44	62	64	68	69	69	108
MC	15.7	18	24	25	26	28	31	41	52	60	63	65	69	73	74	74	11.6
WCR	329	0.38	1.8	3.4	4.9	6.4	9.1	14	26	44	62	71	74	78	79	80	265
WCG	285	0.16	1.2	2.8	4.1	5.7	8.2	13	24	43	62	73	76	79	81	82	234

Data Stationarity

Trend analysis of peak streamflow, date of peak flow and annual water yield among the watersheds shows that all records are stationary, exhibiting no temporal trends ($\alpha \leq 0.05$) (Figure 4 and Table 5). To highlight hydrologic variability, mean peak streamflow (18.2 cms), mean peak streamflow timing (Julian date 141.1) and water yield (20.8 cm/year) were calculated for the watershed Willow Creek above Willow Creek Reservoir (WCR) from 1990-2012 (Figure 5). Departure from the mean for peak streamflow, date of peak streamflow and water yield were plotted around the mean (Figure 5). Cumulative MPB killed area is also plotted here.

Change-point Analysis

Since there were no trends in peak streamflow, date of peak flow or water yield, no significant change-points were detected among the watersheds during the period of record.

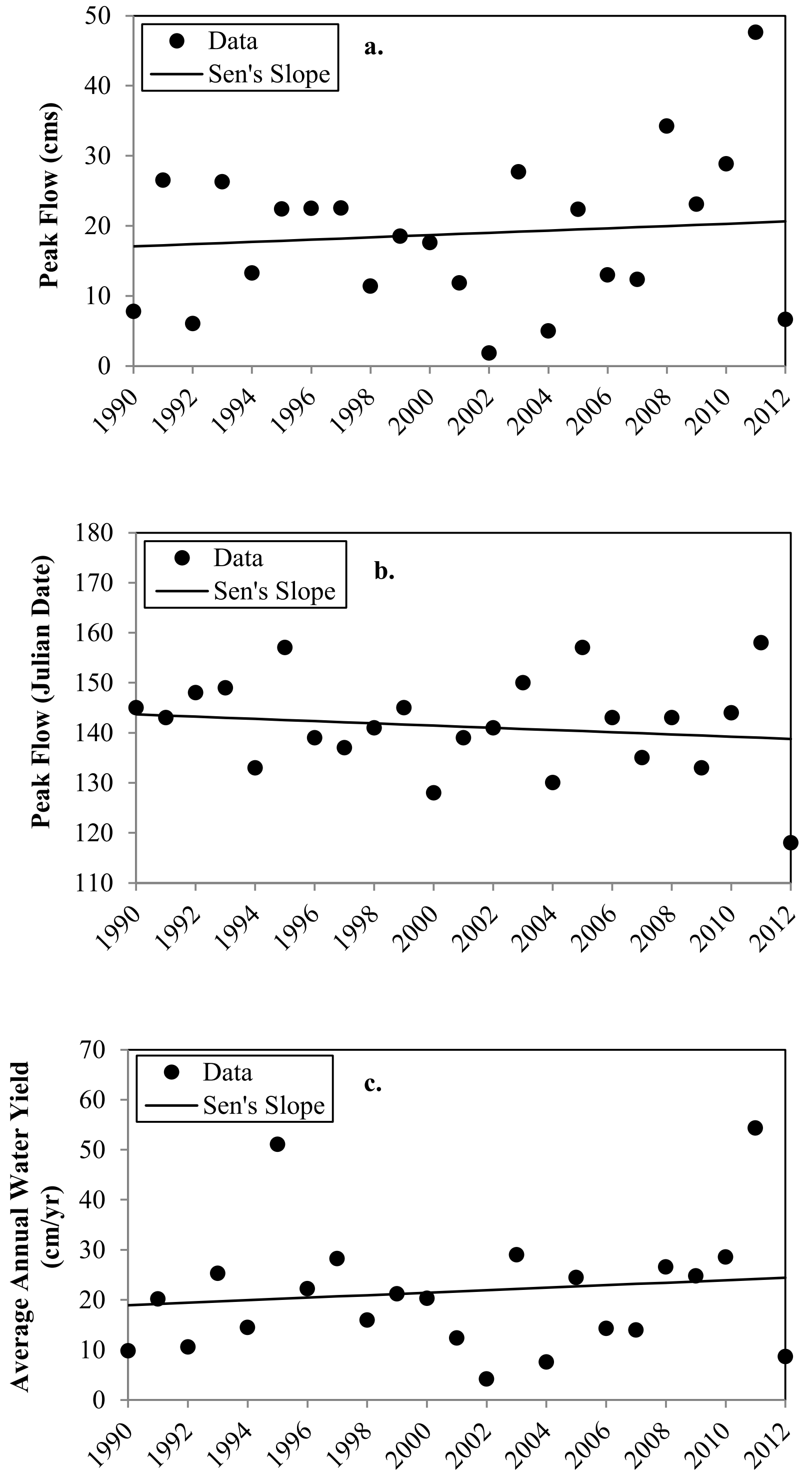

Figure 4. Distribution of data for (a) peak streamflow, (b) date of peak streamflow and (c) annual water yield, as well as the Sen's slope estimate for watershed Willow Creek above Willow Creek Reservoir (WCR). Slope estimates were not statistically significant at $\alpha \leq 0.05$.

Table 5. Results of data-stationarity analysis. For n ≥ 10 a Z-test statistic was used, for n < 10 an S-test statistic was used. Watersheds did not exhibit significant trends (no significance, ns) for peak streamflow, date of peak streamflow, or water yield during the period of record.

				Peak Streamflow (cms)			Peak Streamflow (Julian Day)			Water Yield (cm/year)		
Location	Period of Record (Water Years)		n	Statistic	Q	Significance	Statistic	Q	Significance	Statistic	Q	Significance
EFER	2003	2012	10	1.25	0.33	ns	1.61	3.86	ns	1.25	1.68	ns
SR	1990	2012	23	-0.90	-0.18	ns	-0.45	-0.13	ns	-0.11	-0.12	ns
TC	1990	2012	23	0.16	0.11	ns	-1.16	-0.50	ns	0.00	0.02	ns
WFDC	1990	2012	23	0.61	0.11	ns	0.29	0.20	ns	0.11	0.07	ns
FRUS	1990	2012	23	0.24	0.01	ns	0.67	0.22	ns	0.00	0.00	ns
GC	1990	2012	23	0.77	0.15	ns	-0.63	-0.50	ns	-0.40	-0.38	ns
BC	1990	2012	23	0.66	0.04	ns	-0.42	-0.23	ns	0.11	0.08	ns
WFL	1990	2012	23	0.53	0.22	ns	0.53	0.22	ns	0.48	0.27	ns
FRWP	1990	2012	23	0.00	0.00	ns	0.90	0.36	ns	-0.24	-0.08	ns
WFP	1990	2012	23	1.11	0.55	ns	-0.88	-0.38	ns	0.95	0.49	ns
SFWF	1990	2012	23	-0.63	-0.04	ns	0.69	0.31	ns	0.79	0.30	ns
CC	1990	2012	23	0.61	0.04	ns	0.74	0.50	ns	-0.95	-0.37	ns
KG	1990	2012	23	-0.32	-0.01	ns	-1.83	-0.85	ns	-0.21	-0.13	ns
BCA	1990	2012	23	-0.58	-0.02	ns	0.00	0.00	ns	0.11	0.05	ns
SC	1990	2012	23	-0.03	0.00	ns	-0.11	-0.11	ns	0.79	0.40	ns
RCF	1990	2012	23	0.69	0.11	ns	0.45	0.25	ns	0.48	0.22	ns
SLC	1990	2012	23	0.21	0.11	ns	0.77	0.33	ns	0.32	0.17	ns
RCT	1998	2005	8	*-2.00**	-0.48	ns	*-6.00**	-1.21	ns	*4.00**	0.83	ns
MC	1990	2012	23	0.00	0.00	ns	-0.56	-0.17	ns	0.74	0.15	ns
WCR	1990	2012	23	0.74	0.16	ns	-0.58	-0.22	ns	0.74	0.25	ns

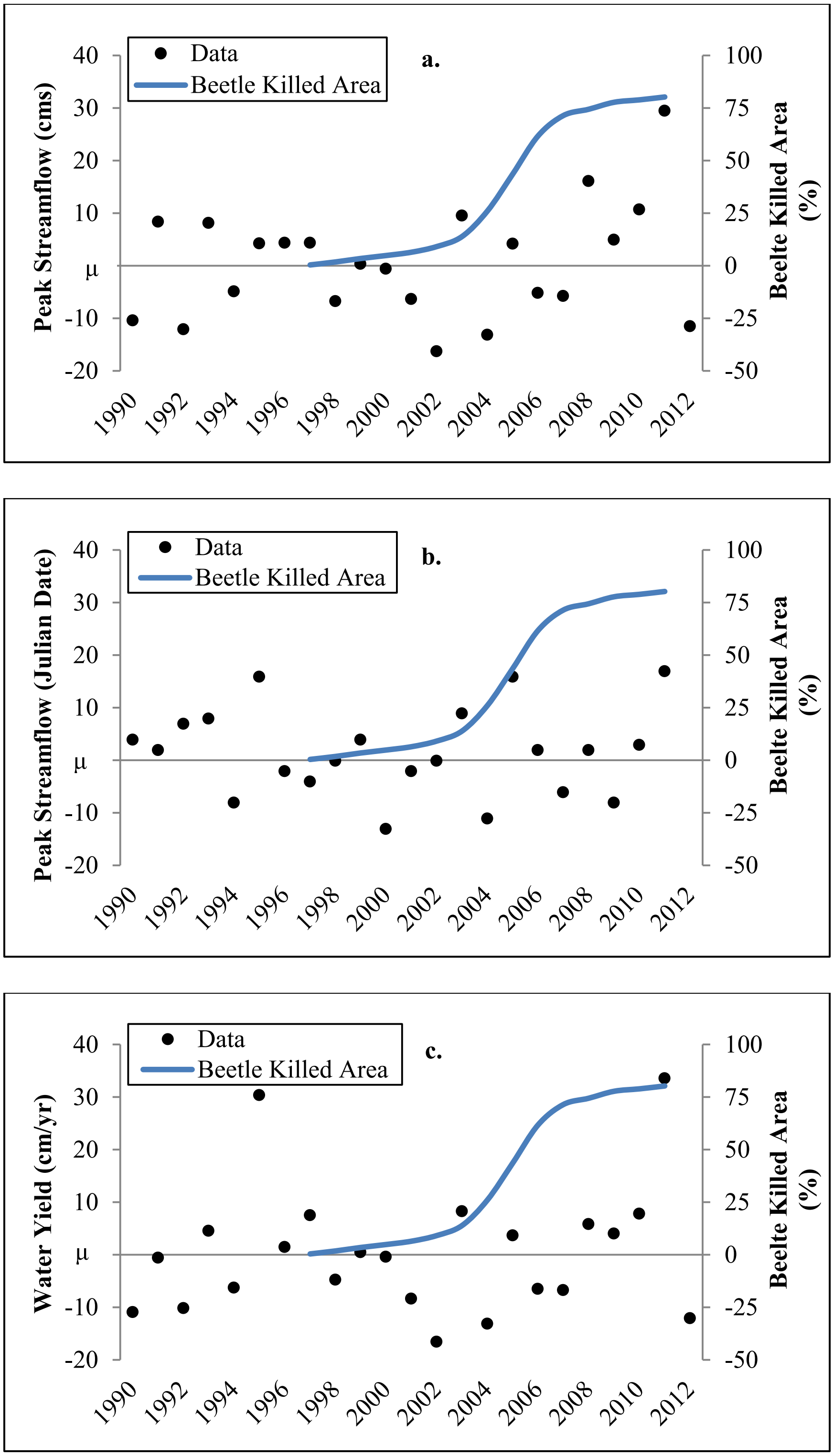

Figure 5. Distribution of residual values (data-mean) for (a) peak streamflow, (b) date of peak streamflow and (c) annual water yield around the mean (μ) for watershed WCR.

Isotopy

A LMWL was developed from snow and rain samples taken within the study area. The LMWL aligns well with the GMWL as well as the Rocky Mountain Meteoric Water Line (RMMWL) (A. Mast personal communication) (Figure 6). A plot of all water samples shows grouping of samples by precipitation type (Figure 7). Location of the snow samples on the LMWL is the result of heavy isotope (^{18}O and ^{2}H) depletion compared to the rain samples. This seasonal or temperature effect is explained by the same processes that account for the latitude effect in isotopes, through which moisture condensation at cooler temperatures produces water that is more depleted of heavy isotopes (Dansgaard 1964). Streamflow samples generally occur on the LMWL. Many of the groundwater samples exhibit a departure from the LMWL. A linear line of best fit, also known as an evaporation line, gives a slope less than that of the LMWL, as well as a lower d-*excess* value. The evaporation line indicates the fractionation of water between the vapor and the residual water. The residual water occurs on the evaporation line below (right of) the LMWL (Ingraham 1998).

Distribution of rain and snow isotopic concentrations from samples taken across the study area shows grouping of samples by collection date and precipitation type (rain versus snow (Figure 8). This grouping is the result of temperature effects on the fractionation of water molecules in the precipitation.

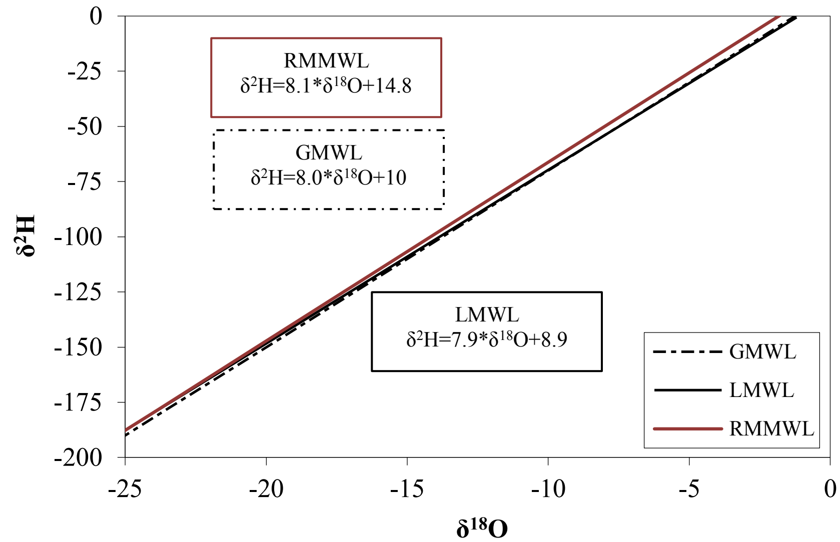

Figure 6. Rocky Mountain Meteoric Water Line, Global Meteoric Water Line and Local Meteoric Water Line are shown.

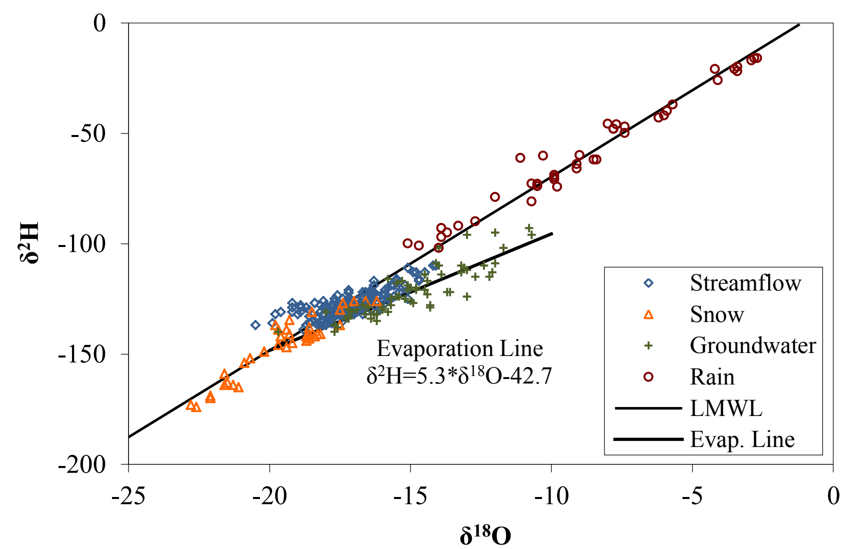

Figure 7. Isotopic composition of streamflow, snow, groundwater and rain samples acquired from all sites. The LMWL and evaporation lines (r^2=0.765) are shown.

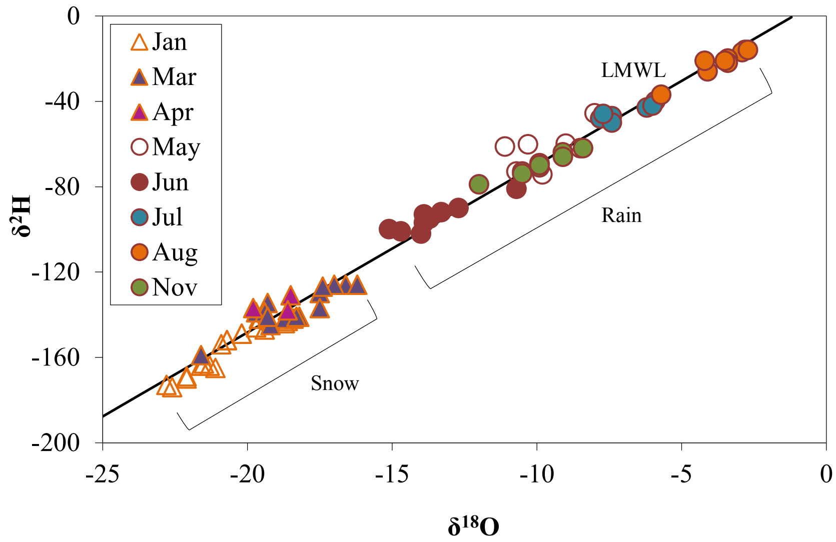

Figure 8. Isotopic composition of precipitation from all sites by sampling date shows little effect on spatial distribution; however seasonal effects in isotopic composition of precipitation samples can be seen.

A closer look at the distribution of streamflow samples shows temporal variation (Figure 9). Most of the streamflow samples fall on the LMWL throughout the sampling season. A comparison of streamflow samples in October and November 2011 to those collected in August and November 2012 show a departure of the August and November 2012 samples from the LMWL. These samples in August and November 2012 experienced enrichment of heavy isotopes compared to streamflow samples taken during October and November 2011 indicating a greater influence of source waters undergoing evaporative effects in August and November 2012. Location of samples below the LMWL indicates a possible influence of water subjected to evaporative effects. Chronological observation of streamflow samples through the study shows enrichment of heavy isotopes from October 2011 through November 2012, as exhibited by migration of streamflow samples up and away from the LMWL.

Mean annual isotopic signatures for snow and rain samples for the study area were used in place of watershed specific mean annual signatures due to evidence of little spatial variation in isotopic composition of precipitation samples between sampling locations (Figure 8), spatial distribution of precipitation collectors and low snow and rain sample numbers in individual watersheds. Mean annual isotopic streamflow and groundwater signatures were developed for each watershed from watershed specific streamflow and groundwater samples (Table 6).

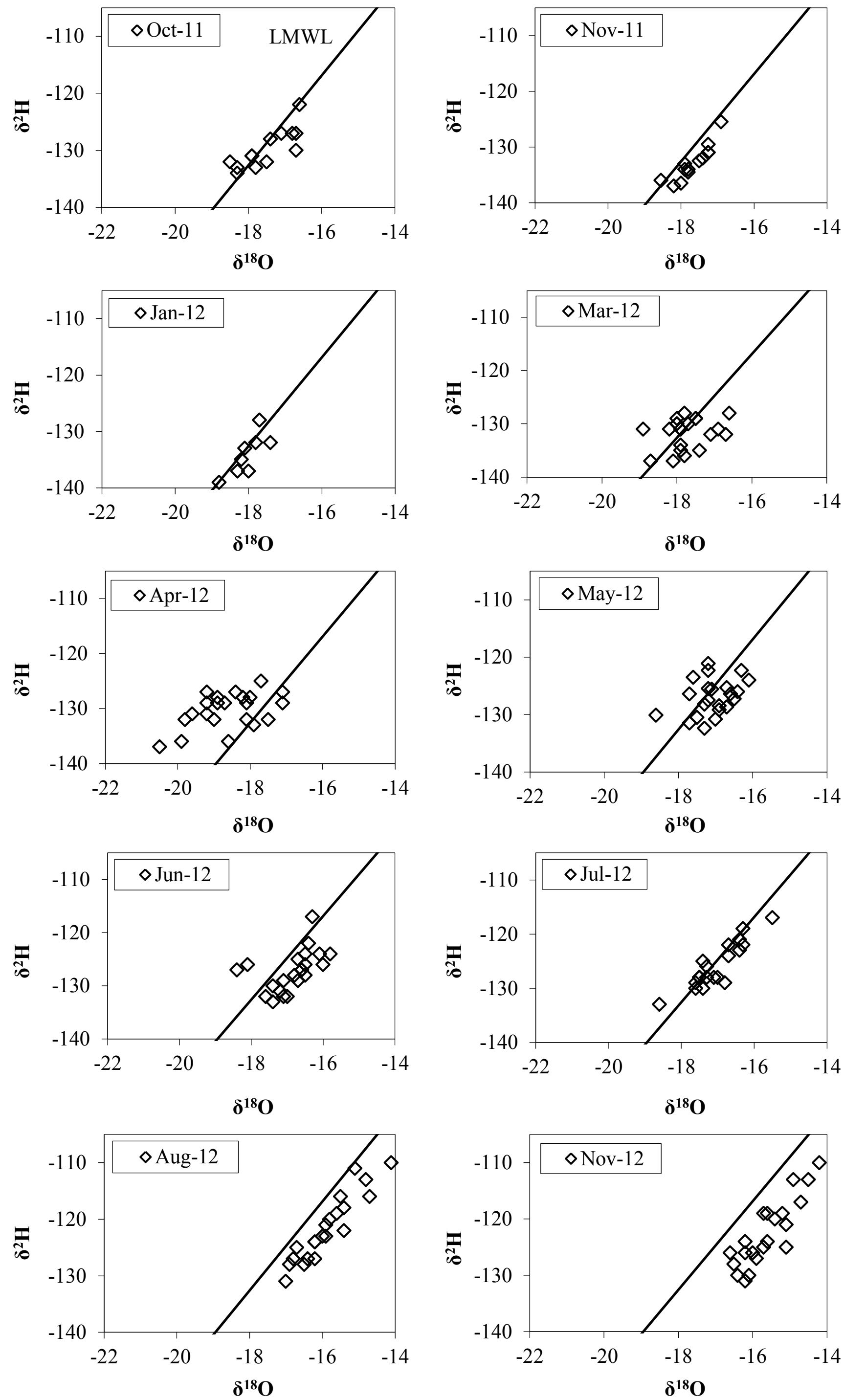

Figure 9. Temporal distribution of streamflow samples.

Table 6. Watershed specific mean isotope concentrations for each sample type for October 2011- November 2012. Sample number, δ^2H, δ^{18}O and *d*-excess are shown. Snow and rain sample types reflect mean isotope concentrations for samples collected over the entire study area.

	Streamflow				Snow				Groundwater				Rain			
Location	**n**	**δ^2H**	**δ^{18}O**	***d*-excess**	**n**	**δ^2H**	**δ^{18}O**	***d*-excess**	**n**	**δ^2H**	**δ^{18}O**	***d*-excess**	**n**	**δ^2H**	**δ^{18}O**	***d*-excess**
WCP					39	-146.3	-19.6	10.3	3	-119.0	-14.5	-3.0	42	-58.9	-8.8	11.1
EFER	6	-131.1	-17.5	8.8	39	-146.3	-19.6	10.3	3	-117.3	-15.7	8.0	42	-58.9	-8.8	11.1
SR	9	-127.1	-17.1	9.8	39	-146.3	-19.6	10.3	3	-120.3	-14.8	-1.9	42	-58.9	-8.8	11.1
TC	9	-128.3	-17.0	8.0	39	-146.3	-19.6	10.3	3	-125.0	-15.6	0.1	42	-58.9	-8.8	11.1
WFDC	10	-129.7	-17.4	9.8	39	-146.3	-19.6	10.3	3	-129.3	-15.9	-2.1	42	-58.9	-8.8	11.1
FRUS	8	-129.8	-17.6	10.8	39	-146.3	-19.6	10.3	3	-107.0	-14.0	5.3	42	-58.9	-8.8	11.1
GC	9	-108.6	-14.7	9.2	39	-146.3	-19.6	10.3	3	-130.3	-16.4	0.6	42	-58.9	-8.8	11.1
BC	8	-122.5	-16.8	12.2	39	-146.3	-19.6	10.3	3	-122.7	-15.3	-0.3	42	-58.9	-8.8	11.1
WFL	8	-130.4	-17.2	6.9	39	-146.3	-19.6	10.3	3	-131.0	-17.0	5.3	42	-58.9	-8.8	11.1
FRWP	7	-128.2	-17.3	9.9	39	-146.3	-19.6	10.3	3	-125.0	-14.4	-10.1	42	-58.9	-8.8	11.1
WFP	9	-128.7	-17.0	7.5	39	-146.3	-19.6	10.3	4	-115.5	-14.6	1.1	42	-58.9	-8.8	11.1
SFWF	10	-132.2	-17.7	9.2	39	-146.3	-19.6	10.3	3	-115.7	-13.4	-8.7	42	-58.9	-8.8	11.1
CC	9	-122.2	-16.9	12.9	39	-146.3	-19.6	10.3	3	-130.3	-17.4	8.6	42	-58.9	-8.8	11.1
KG	8	-131.5	-17.6	9.3	39	-146.3	-19.6	10.3	3	-113.7	-12.9	-10.2	42	-58.9	-8.8	11.1
BCA	8	-123.1	-16.5	9.0	39	-146.3	-19.6	10.3	3	-107.3	-13.1	-2.3	42	-58.9	-8.8	11.1
SC	10	-134.4	-17.9	9.1	39	-146.3	-19.6	10.3	3	-125.7	-14.3	-11.5	42	-58.9	-8.8	11.1
RCF	10	-124.3	-16.9	10.5	39	-146.3	-19.6	10.3	3	-119.0	-13.7	-9.7	42	-58.9	-8.8	11.1
SLC	10	-130.2	-17.3	8.5	39	-146.3	-19.6	10.3	3	-133.3	-16.7	0.0	42	-58.9	-8.8	11.1
RCT	9	-123.3	-16.3	7.4	39	-146.3	-19.6	10.3	3	-128.7	-16.1	0.4	42	-58.9	-8.8	11.1
MC	7	-125.6	-16.8	9.0	39	-146.3	-19.6	10.3	3	-124.3	-15.6	0.2	42	-58.9	-8.8	11.1
WCR	9	-126.4	-16.9	9.0	39	-146.3	-19.6	10.3	3	-122.7	-14.5	-6.4	42	-58.9	-8.8	11.1

Distribution of d-*excess* values illustrates the influence of evaporative effects. Lower d-*excess* values are indicative of increasing evaporative effects on samples (Gupta 2010). Groundwater samples had the lowest *d*-excess values because this source water is subjected to greater evaporation than streamflow, snow or rain. Streamflow samples collected in April and May 2012 when groundwater samples were also collected show an increase in *d*-excess. Temporal variation of isotopic composition in streamflow samples can be seen in the distribution of *d*-excess values (Figure 10).

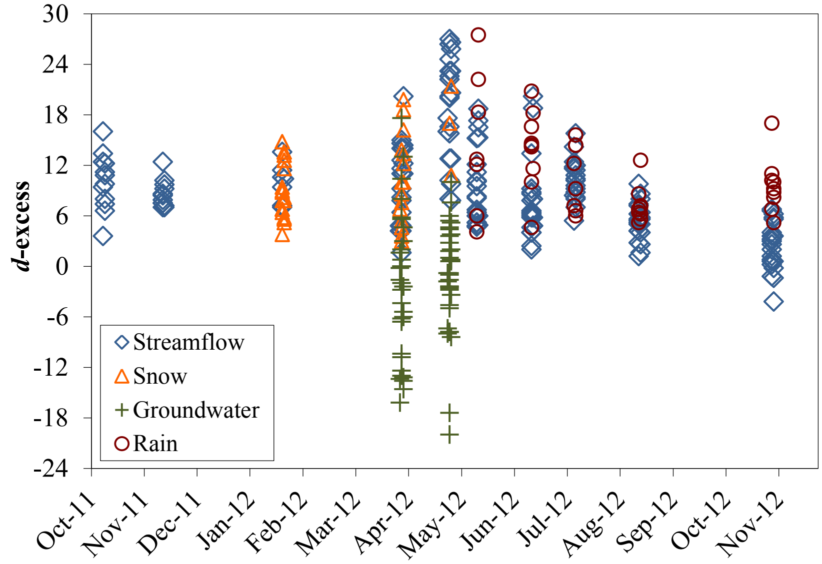

Figure 10. *d*-excess values of streamflow, snow, groundwater and rain samples versus sample date are shown to illustrate increased evaporative effect on groundwater samples.

Streamflow Source Water Separation

Isotopic signatures were used to partition streamflow contributions from snow, rain and groundwater via IsoSource. An increment value of 1% and tolerance value of 0.434‰ (as calculated from equation 5) were used for all watersheds. The tolerance value is calculated as half the increment value times the maximum difference between isotopic signatures of sources. Because IsoSource yields numerous feasible solutions to the mass balance equation, a range of solutions is presented. The solutions were ranked, and shown here are the mean, minimum and maximum viable contributions to streamflow (Figure 11).

Snow makes up the greatest contribution to streamflow in the majority of the study watersheds. Groundwater makes up the second greatest contribution to streamflow, followed by rain. Three watersheds, representing 5, 33 and 39% beetle-killed area, corresponding to EFER, GC and WFL watersheds respectively (Figure 11a) do not see the greatest contribution of streamflow coming from snow. The watersheds representing 5 and 39% beetle-killed area (EFER and WFL) have a larger fraction of groundwater to streamflow than from snow or rain; however the range of possible source contributions in these watersheds is large: EFER (snow = 0.00-0.61, groundwater = 0.00-0.92, rain = 0.08-0.39) and WFL (snow = 0.00-0.81, groundwater = 0.01-0.99, rain = 0.01-0.18). The watershed representing 33% beetle-killed area (GC) is estimated to have contributed more rain to streamflow than snow and groundwater during the investigation, again, the range of source contributions is large: GC (snow = 0.12-0.57, groundwater = 0.00-0.55, rain = 0.33-0.43).

Linear regression of mean source water contributions to streamflow and 2012 MPB killed area (Figure 11a) yields a positive linear relationship ($y= 0.0015x+0.53$, $r^2= 0.053$) between beetle-killed area and snow contribution to streamflow; a negative linear relationship (y= -

0.0012x+0.29, r^2= 0.043) between beetle-killed area and groundwater contribution to streamflow; and a negative linear relation (y= -0.00030x+0.19, r^2= 0.010) between beetle-killed area and rain contribution to streamflow.

To assess the strength of relations between mean contribution to streamflow from source waters and 2012 beetle-killed area Spearman's correlation coefficient was used. First a Spearman correlation coefficient (rs) (Eq. 6) was calculated from raw data (X_i and Y_i), which was converted to ranked values (x_i and y_i). This equation allows for tied values.

$$r_s = \frac{\sum_i (x_i - \bar{x})(y_i - \bar{y})}{\sqrt{\sum_i (x_i - \bar{x})^2 \sum_i (y_i - \bar{y})^2}} \quad (6)$$

The Spearman coefficient was the used to calculate a critical t-value (Eq. 7) where d.f. is the sample number minus 2.

$$t = \frac{r_s}{sqrt(\frac{1 - {r_s}^2}{d.f})} \quad (7)$$

The associated risk (p-value) was determined from the t-value.

Results from the Spearman correlation coefficient test show that correlations between mean contribution to streamflow from source waters and 2012 MPB killed area are not statistically significant at $\alpha > 0.05$ (Table 7).

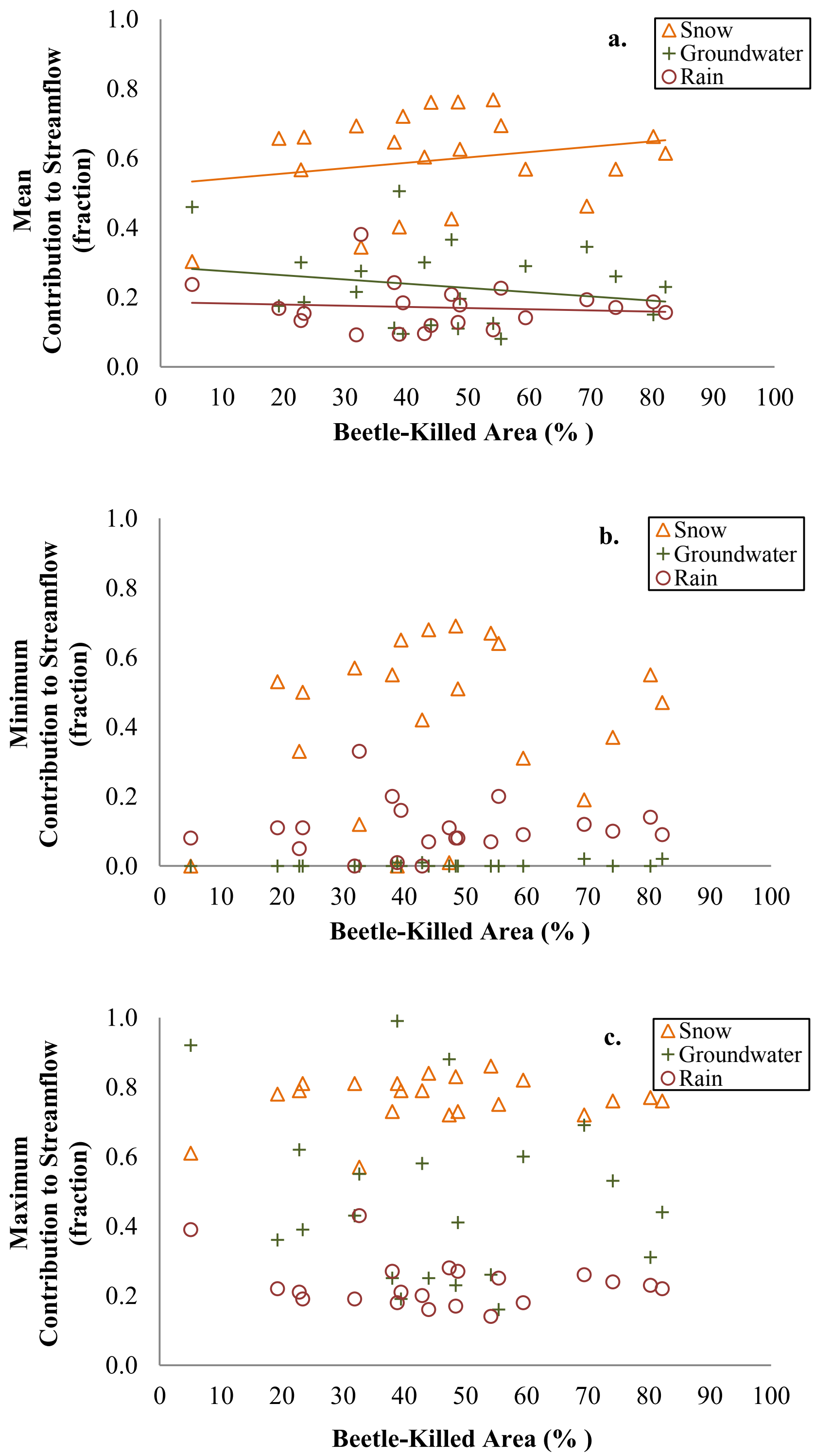

Figure 11. (a)Mean, (b) minimum and (c) maximum estimated snow, groundwater and rain source water contributions to streamflow (fraction), as determined from IsoSource.

Table 7. Parameters describing statistical strength of relations between mean source contributions to streamflow and beetle-killed area (%). Represented are sample number (n), correlation coefficient (r_s), t-value, degrees of freedom (df), and p-value.

	Beetle-Killed Area				
	n	**r_s**	**t-value**	**df**	**p-value**
Snow	21	0.126	0.560	19	0.582
Soilwater	21	-0.141	-0.62	19	0.543
Rain	21	0.030	0.13	19	0.897

DISCUSSION

Mountain Pine Beetle

MPB killed watershed area ranged from 5 to 82%. A large number of watersheds were chosen for the study due to the difficulty in finding watersheds of similar sizes with comparative characteristics and active stream gauges that represented a range of beetle-killed areas. Most of Colorado has been subjected to extensive MPB attack with minimally affected watersheds challenging to find. Thus, minimally impacted watersheds may be underrepresented. While this is true, the study watersheds represent low to severe MPB impact.

Area of MPB kill determined from aerial detection surveys characterizes forest health only by what can be detected from above the forest canopy. This method accounts for tree mortality as determined by crown characterization, and does not account for understory growth or tree regrowth that often cannot be seen from above. As a result, assessment of forest health based solely on aerial detection surveys may overestimate the degree for forest mortality by overlooking understory growth.

The age of forest mortality, based on the aerial detection surveys, indicates the majority of dead trees in these watersheds are in the gray tree phase which occurs approximately three years after the initial attack (British Ministry of Forests 1995). These trees, devoid of needles, have decreased ability to intercept falling precipitation, decreased ET, and allow increase radiation transmission to the forest floor (Pugh and Small 2011). While gray phase forests bring about hydrologic changes similar to those seen in forests subjected to timber harvesting, unlike timber harvesting, most of these gray phase trees in the study watersheds remain standing. In addition to complete tree removal, timber harvesting may cause damage to the understory which may be not seen in MPB affected forests (Boon 2008). These factors may lead to the difference between hydrologic responses to timber harvesting and MPB mortality.

Data Stationarity and Change-point Analysis

Daily streamflow and annual peak streamflow data were used without corrections for diversions. The forested watersheds are largely on federal lands with little no to land use change over time. The Mann-Kendall test for data stationarity showed no statistically significant ($\alpha \leq 0.05$) trends in peak flow, date of peak flow or annual water yield during the period of record. Due to the lack of trends in the data, change-point tests were omitted.

The determination of data stationarity of hydrologic records for the study watersheds is contradictory to findings of increased water yield in MPB affected watersheds (Love 1955; Bethlahmy 1974; Bethlahmy 1975; Potts 1984). Increased water yield was observed during and post MPB attack in the White River Basin in Colorado (Love 1955). Further research showed increased water yield over the next 15 years post-attack in the same watershed (Bethlahmy 1974, 1975). This extended period of increased water yield was partially attributed to a lack for forest regrowth in many areas of the affected watershed (Bethlahmy 1974, 1975). Increased water yield in the Jack Creek watershed in Montana was observed as a result of the mid 1970 MPB infestation (Potts 1984). Five years post-attack, increased water yield, increased low flows and earlier peak flows were observed (Potts 1984). Evidence of advancing snowmelt and snowmelt runoff between 1978 and 2007 has also been seen in Colorado (Clow 2010), contradicting observed peak flow date stationarity.

Differing local climatic and meteoric conditions attributed to different study area and study year, as well as differing forest composition compared to the studies above are possible factors resulting in a lack of hydrologic response observed in the long term streamflow records for the study watersheds. Recent warming trends have led to decreased duration of snow cover and decreased maximum SWE in Colorado (Clow 2010; Harpold et al. 2012). Because this study was conducted during a period when precipitation, SWE and thus streamflows were particularly low (Figures 2 and 4) these low data on the tail-end of the record may show minimal response to watershed changes and thus affect stationarity of the hydrologic data. Forest composition, including unaccounted understory regrowth, may also be a factor in the differences observed between historic studies on hydrologic responses to MPB attack and this study.

Land surface changes including the removal of felled trees and damage or removal of undergrowth associated with timber harvesting does not accompany MPB attack. These differences in land surface disturbance may account for the differences in hydrologic responses to timber harvesting and MPB attack. While interception in beetle-killed forests decreases along with ET (Troendle and King 1985; Troendle 1987; Troendle and Ruess 1997; Winkler et al. 2005), the branches and twigs remaining on a MPB attacked tree may still intercept snowfall and limit transmission of incoming solar radiation to the snow or soil surface. This creates conditions dissimilar to those occurring in timber harvested forests where trees are felled and removed. These land surface and forest alterations are factors contributing to hydrologic responses of increased water yield observed in watersheds where timber harvesting was occurring (Stednick 1996). Marked hydrological responses of increased water yield and some peak flows in timber-harvested watersheds (Stednick 1996) were not seen in these MPB affected watersheds.

Isotopy

Stable isotopes, ^{2}H and ^{18}O, of water were used to identify isotope signatures of streamflow and its source waters. A LWML was developed from precipitation samples, as snow and rain, collected from the study area (Figure 7). Source water samples were distributed along the LMWL as expected. Differing location of snow and rain samples on the LMWL is a result of the temperature effect on stable isotopes of water, whereby water condensing at cooler temperatures is increasingly depleted of heavy isotopes (Dansgaard 1964). Snow samples, which occur further down the LMWL, are depleted in heavy isotopes relative to rain samples, which occur further up the LWML. Groundwater sample occurred below (to the right of) the LMWL as a result of isotopic fractionation during evaporation (Gupta 2010). Departure from the LMWL indicates decreasing *d*-excess values, implying that ^{18}O is preferentially enriched in heavy isotopes compared to ^{2}H. This preferential enriched of ^{18}O is a result of evaporative effects (Gupta 2010).

Isotopic concentrations of streamflow by sampling date (Figure 9) exhibit movement up the LMWL over the course of the study, which may indicate seasonal temperature effects. A comparison of streamflow samples in October and November 2011 to those collected in August and November 2012 show a departure of the August and November 2012 samples from the LMWL. These samples in August and November 2012 experienced less depletion of heavy isotopes than streamflow samples taken during October and November 2011. Location of these samples below the LMWL indicates a possible influence of water subjected to evaporative effects. This may signify a greater influence of groundwater on the streamflow samples.

Due little spatial variation in isotopic composition of precipitation samples, a mean annual snow and mean annual rain signature was created for the study area. Mean annual isotopic streamflow and groundwater signatures were developed for each watershed from watershed specific streamflow and groundwater samples. Annual values were used since one of the test parameters is annual water yield.

Streamflow Source Water Separation

Fractionation of isotopes during phase changes of water creates unique isotopic signatures for each phase of water (Kendall and Caldwell 1998). Isotopic analysis of streamflow source waters of snow, rain and groundwater, collected from study watersheds show distinct source water signatures allowing for use in the IsoSource multi-source mixing model. Because IsoSource yields numerous feasible solutions, a range of possible solutions were presented (Figure 11). For comparative purposes, the mean of the feasible contributions to streamflow will be considered.

Mean contribution values show snow makes up the greatest contribution to streamflow in 18 of the watersheds. Groundwater makes up the second greatest contribution to streamflow, followed by rain, which contributes the smallest fraction to streamflow (Figure 11a). Three watersheds exhibit non-snow source waters as the primary contributor to streamflow. Additionally, several watersheds show negligible differences between groundwater and rain contributions to streamflow.

The contribution of streamflow coming from snow increases with increasing beetle-killed area; the fraction of streamflow contributed from groundwater decreases with increasing beetle-killed area; and the fraction of streamflow coming from rain remains nearly constant with increasing beetle-killed area; however none of these correlations were statistically significant (Table 7). In general, during the 2012 water year, source water contributions to streamflow were: snow 60%, groundwater 20% and rain 20% (Figure 11a).

CONCLUSIONS

The mountain pine beetle (MPB) outbreak of the 1990's in Colorado has killed extensive areas of lodgepole pine forest. While the rate of MPB caused mortality has decreased in recent years, large areas of dead forest remain. In north-central Colorado 21 watersheds were chosen for analysis of the effects of MPB caused forest mortality on streamflow and streamflow generation processes. Study watersheds represent 5 to 82% of beetle-killed watershed area.

The Mann-Kendall statistical test was used to confirm data stationarity in peak streamflow, date of peak streamflow and annual water yield. Since there were no trends, change-point analyses were omitted.

Isotopic analysis and accompanying 3-component streamflow source water separation between streamflow sources, snow, groundwater and rain, indicate source contributions to streamflow did not significantly change with increasing beetle-killed area. In general, source water contributions to streamflow are partitioned by the following; snow 60%, groundwater 20% and rain 20%. These estimations are based on the mean contributions calculated from mean 2012 isotopic signatures of source waters for each watershed in this study.

The results of this study showed that MPB does not affect peak streamflow, date of peak streamflow or annual water yield. Isotopic analysis of streamflow source waters show that MPB does not affect streamflow generation mechanisms, source water contributions to streamflow did not change with increasing beetle-killed area.

RECOMMENDATIONS

This study showed that MPB killed forests had no effect on streamflow as measured by peak streamflow, date of peak streamflow and water yield, or streamflow generation mechanisms as measured by streamflow source waters. Minimally affected watersheds (< 20% watershed area killed) were underrepresented. Research shows that measureable changes in streamflow on a watershed scale cannot be determined from hydrologic records when less than 20% of the watershed has been harvested, or beetle-killed in the case of this study. A greater number of minimally impacted watersheds would have aided in the comparison of hydrologic changes. While it may be hard to accomplish due to the extent of MPB infestation in Colorado, a paired watershed study could serve to better control inherent differences in watershed characteristics. If paired watersheds cannot be found, better representation of minimally affected watersheds could help to strengthen a comparison between minimally affected watersheds and heavily affected watersheds.

The use of stable isotopes as environmental tracers provided unique source water tracer signatures, easily utilized in hydrograph separation. An improved sampling scheme to include year round sampling of groundwater would provide more robust evidence of a groundwater influence on streamflow during low flow periods. An assumption of a suitable correlation between groundwater and groundwater was made in this study. It was assumed that groundwater could be used as a surrogate for groundwater based on decreased evaporative effects with depth. It was also assumed that due to a lack of groundwater recharge necessary in dead stands, excess groundwater was seeping into groundwater stores which then traveled to the stream channel.

Sampling of groundwater would be useful in determining if a connection between groundwater and groundwater does exist, and their effects on streamflow generation.

LITERATURE CITED

Bethlahmy N. 1974. More streamflow after a bark beetle epidemic. Journal of Hydrology 23(3-4):185-189.

Bethlahmy N. 1975. A Colorado episode: beetle epidemic, ghost forests, more streamflow. Northwest Science 49(2):95-105.

Boon S. 2007. Snow accumulation and ablation in a beetle-killed pine stand in Northern Interior British Columbia. BC Journal of Ecosystems and Management 8(42):1-13. Available from: http://www.forrex.org/publications/jem/ISS42/vol8_no3_art1.pdf Accessed 11 Oct 2012.

Boon S. 2008. Impact of mountain pine beetle infestation and salvage harvesting on seasonal snow melt and runoff. Mountain pine beetle working paper 2008-24. Alberta, CA: University of Lethbridge. p 28.

British Columbia Ministry of Forests. 1995. Bark beetle management guidebook. Forest practices code. Victoria, BC. Forest Practices Branch. Available from: http://www.for.gov.bc.ca/tasb/legsregs/fpc/fpcguide/beetle/betletoc.htm Accessed 08 Nov 2011.

Buttle J. 2005. Isotope hydrograph separation of runoff sources. Encyclopedia of Hydrological Sciences. p.1-12. Available from: http://onlinelibrary.wiley.com/doi/10.1002/0470848944.hsa120/pdf Accessed 02 Oct 2012.

Carroll A, Taylor S, Regniere J, Safranyik L, Shore T, Brooks J, Stone J. 2004. Effects of climate change on range expansion by the mountain pine beetle in British Columbia. Mountain Pine Beetle Symposium: Challenges and Solutions 399:223-232.

Clow, D. W. 2010. Changes in the timing of snowmelt and streamflow in Colorado: A response to recent warming. Journal of Climate. 23: 2293–2306. doi:10.1175/2009JCLI2951.1.

Colorado State Forest Service (CSFS). 2011 Report on the Health of Colorado's Forests. Available from: http://csfs.colostate.edu/pdfs/126850_2011HealthColoForest-www.pdf Accessed 11 Apr 2012.

Colorado Water Conservation Board (CWCB). 2010. Colorado's Water Supply Future: State of Colorado 2050 Municipal and Industrial Water Use Projections. Available from: http://cospl.coalliance.org/fedora/repository/co:9366/nr32f982010internet.pdf

Cooper LW. 1998. Isotopic Fractionation in Snow Cover. In: Kendall C, McDonnell JJ, editors. Isotope Tracers in Catchment Hydrology. Amsterdam: Elsevier. p. 119-136.

Dansgaard W. 1964. Stable isotopes in precipitation. Tellus 16(4):436-468.

Dawson T, Simonin K. 2011. The Roles of Stable Isotopes in Forest Hydrology and Biogeochemistry. In: Levia DF, Carlyle-Moses D, Tanaka T, editors. Forest Hydrology and Biogeochemistry. Netherlands: Springer. p. 137-161.

Earth System Research Laboratory (ESRL). Boulder, Colorado Climate and Weather Data. www.esrl.noaa.gov/psd/boulder/ Accessed 25 Aug 2012.

Fettig C, Klepzig K, Billings R, Munson A, Nebeker T, Negron J, Nowak J. 2007. The effectiveness of vegetation management practices for prevention and control of bark beetle infestations in coniferous forests of the western and southern United States. Forest Ecology and Management 238(1-3):24-53.

Gat JR. 2010. Isotope Hydrology: A Study of the Water Cycle. London: Imperial College Press. p. 189.

Gilbert R. 1987. Statistical Methods for Environmental Pollution Monitoring. New York: John Wiley & Sons, Inc. p. 208-224

Gupta S. 2010. Modern Hydrology and Sustainable Water Development. United Kingdom: Wiley-Blackwell. p. 450.

Harpold A., Brooks P., Rajagopal S., Heidbuchel I., Jardine A., Stielstra C. 2012. Changes in snowpack accumulation and ablation in the intermountain west. Water Resources Research. 48(11501): 11 pp. doi:10.1029/2012WR011949.

Hélie JF, Peters DL, Tattrie KR, Gibson JJ. 2005. Review and synthesis of potential hydrologic impacts of mountain pine beetle and related harvesting activities in British Columbia. Mountain pine beetle initiative working paper 2005-23. Canada: Canadian Forest Service.

Hubbard R, Rhoades C, Elder K, Negron J. 2013. Changes in transpiration and foliage growth in lodgepole pine trees following mountain pine beetle attack and mechanical girdling. Forest Ecology and Management 289:312-317.

Ingraham NL. 1998. Isotopic Variations in Precipitation. In: Kendall C, McDonnell JJ, editors. Isotope Tracers in Catchment Hydrology. Amsterdam: Elsevier. p. 87-118.

International Atomic Energy Agency (IAEA). 1997. Technical procedure for cumulative monthly sampling of precipitation for isotopic analysis. Available from: http://www-naweb.iaea.org/NAALIHL/docs/tech_info/Precipitation%20Sampling97.pdf Accessed 09 Nov 2012.

Jouzel J, Merlivat L. 1984. Deuterium and O-18 in precipitation- modeling of the isotopic effects during snow formation. Journal of Geophysical Research-Atmospheres 89(ND7):1749-1757.

Kendall C, Caldwell EA. 1998. Fundamentals of Isotope Geochemistry. In: Kendall C, McDonnell JJ, editors. Isotope Tracers in Catchment Hydrology. Amsterdam: Elsevier. p. 51-86.

Leaf C. 1975. Watershed management in the Rocky Mountain subalpine zone: the status of our knowledge. Rocky Mountain Forest and Range Experiment Station
USDA Forest Service. p. 31.

Love L. 1955. The effect on stream flow of the killing of spruce and pine by the Englemann spruce beetle. Transactions of the American Geophysical Union 36:113-118.

Ma Z, Kang S, Zhang L, Tong L, Su X. 2008. Analysis of impacts of climate variability and human activity on streamflow for a river basin in arid region of northwest China. Journal of Hydrology 352(3-4):239-249.

MacDonald LH, Stednick JD. 2003. Forests and Water: A State-of-the-Art Review for Colorado. CWRRI Completion Report 196. Colorado, USA: Colorado State University. p. 65.

Man, Gary. 2012. Major Forest Insect and Disease Conditions in the United States: 2011. USDA Forest Service. Report No: FS-1000.

Mast, A. USGS-Denver. Personal communication. 2013.

Milly P, Betancourt J, Falkenmark M, Hirsch R, Kundzewicz Z, Lettenmaier D, Stouffer R. 2008. Stationarity is dead: wither water management. Science 318:573-574.

Pettitt A. 1979. A nonparametric approach to the change-point problem. Applied Statistics 28(2):126-135.

Phillips D, Gregg J. 2003. Source partitioning using stable isotopes: coping with too many sources. Oecologia 136:261-269.

Potts D. 1984. Hydrologic impacts of a large-scale mountain pine-beetle (*Dendroctonus-ponderosae* Hokpins) epidemic. Water Resources Bulletin 20(3):373-377.

Pugh E, Small E. 2011. The impact of pine beetle infestation on snow accumulation and melt in the headwaters of the Colorado River. Ecohydrology. DOI 10.1002/eco.239

Rao AR, Hamed KH, Chen H-L. 2003. Nonstationarities in Hydrologic and Environmental Time Series. Dordrecht, The Netherlands: Kluwer Academic Publishers. p. 362.

Rodhe A. 1998. Snowmelt-Dominated Systems. In: Kendall C, McDonnell JJ, editors. Isotope Tracers in Catchment Hydrology. Amsterdam: Elsevier. p. 391-434.

Rouse WR. 1984. Microclimate at the arctic tree line. Radiation balance of tundra and forest. Water Resource Research 20: 57–66.

Safranyik L. Mountain pine beetle: biology overview. In: Proceedings: symposium on the management of lodgepole pine to minimize losses to the mountain pine beetle. Amman GD (editor 1989). Kalispell, Montana: USDA Forest Service, Intermountain Research Station. p. 9-13.

Safranyik L, Carroll, A. L. 2006. The biology and epidemiology of the mountain pine beetle in lodgepole pine forests. The Mountain Pine Beetle A Synthesis of Biology, Management, and Impacts on Lodgepole Pine. Victoria, BC: Canadian Forest Service. p. 3-66.

Salarijazi M, Akhond-Ali A, Adib A, Daneshkhah A. 2012. Trend and change-point detection for the annual stream-flow series of the Karun River at the Ahvaz hydrometric station. African Journal of Agricultural Research 7(32):4540-4552.

Salmi, T., Määttä, A., Anttila, P., Ruoho-Airola, T., and Amnell, T. 2002. Detecting trends of annual values of atmospheric pollutants by the Mann-Kendall test and Sen's slope estimates – the Excel template application MAKESENS. Helsinki, Finnish Meteorlogical Institute. Report Code FMI-AQ-31.

Singh BP, Kumar B. 2005. Isotopes in Hydrology, Hydrogeology and Water Resources. New Delhi: Narosa. p. 188.

Stednick J. 1996. Monitoring the effects of timber harvest on annual water yield. Journal of Hydrology 176(1-4):79-95.

Troendle C. 1987. Effect of clearcutting on streamflow generating processes from a subalpine forest slope. International Association of Hydrological Sciences. p. 545-551.

Troendle C, King R. 1985. The effect of timber harvest on the Fool Creek watershed, 30 years later. Water Resources Research 21(12):1915-1922.

Troendle C, Leaf C. 1981. Effects of timber harvest in the snow zone on volume and timing of water yield. In: Interior West watershed management symposium. Pullman, WA: Washington State University. p. 228.

Troendle C, Reuss J. 1997. Effect of clear cutting on snow accumulation and water outflow at Fraser, Colorado. Hydrology and Earth System Sciences 1(2):325-322.

USDA Forest Service. 2011. Pest Damage Summary: Mountain Pine Beetle. Available from: http://foresthealth.fs.usda.gov/portal/PestSummary/DamageSummary Accessed 01 Nov 2012.

USDA Forest Service. 2012. Rocky Mountain Region 2012 Aerial Detection Survey Results. Available from: http://www.fs.usda.gov/detail/r2/forest-.grasslandhealth/?cid=stelprdb5408531 Accessed 14 Apr 2013

University of Wyoming Stable Isotope Facility. Available from: http://www.uwyo.edu/sif/ Accessed 09 Sept 2012.

Williams M, Losleben M, Caine N, Greenland D. 1996. Changes in climate and hydrochemical responses in a high-elevation catchment in the Rocky Mountains, USA. Limnology and Oceanography 41(5):939-946.

Winkler R, Spittlehouse D, Golding D. 2005. Measured differences in snow accumulation and melt among clearcut, juvenile, and mature forests in southern British Columbia. Hydrological Processes.19:51-62.

Wulder M, White J, Bentz B, Alvarez M, Coops N. 2006. Estimating the probability of mountain pine beetle red-attack damage. Remote Sensing of Environment 101(2):150-166.

Zhang X, Zhang L, Zhao J, Rustomji P, Hairsine P. 2008. Responses of streamflow to changes in climate and land use/cover in the Loess Plateau, China. Water Resources Research 44. DOI:10.1029/2007WR006711

APPENDIX

Table A-1 . Isotope data by location, sample type and sampling date.

USGS #	Location	Sample Type	Sampling Date	δ²H	δ¹⁸O	d-*excess* (‰)
9020000	WCG	STREAMFLOW	10/8/2011	-130	-16.7	3.60
9020000	WCG	STREAMFLOW	11/13/2011	-131	-17.3	7.00
9020000	WCG	SNOW	1/22/2012	-144	-18.7	5.60
9020000	WCG	SNOW	1/22/2012	-143	-18.6	5.80
9020000	WCG	GROUNDWATER	3/30/2012	-113	-12.1	-16.2
9020000	WCG	GROUNDWATER	3/30/2012	-132	-16.3	-1.60
9020000	WCG	STREAMFLOW	3/30/2012	-128	-16.6	4.80
9020000	WCG	GROUNDWATER	4/27/2012	-117	-14.4	-1.80
9020000	WCG	STREAMFLOW	4/27/2012	-128	-18.2	17.6
9020000	WCG	STREAMFLOW	5/14/2012	-125	-16.7	8.30
9020000	WCG	STREAMFLOW	6/15/2012	-128	-16.5	4.00
9020000	WCG	STREAMFLOW	7/10/2012	-122	-16.3	8.40
9020000	WCG	STREAMFLOW	8/17/2012	-123	-16.0	5.00
9020000	WCG	STREAMFLOW	11/3/2012	-126	-16.0	2.00
9020500	WCR	STREAMFLOW	11/13/2011	-132	-17.4	7.20
9020500	WCR	SNOW	1/22/2012	-141	-18.6	7.80
9020500	WCR	SNOW	1/22/2012	-142	-18.4	5.20
9020500	WCR	STREAMFLOW	1/22/2012	-132	-17.8	10.4
9020500	WCR	GROUNDWATER	3/30/2012	-115	-12.7	-13.4
9020500	WCR	GROUNDWATER	3/30/2012	-140	-17.7	1.60
9020500	WCR	STREAMFLOW	3/30/2012	-131	-16.9	4.20
9020500	WCR	GROUNDWATER	4/27/2012	-113	-13.2	-7.40
9020500	WCR	STREAMFLOW	4/27/2012	-128	-18.0	16.0
9020500	WCR	STREAMFLOW	5/14/2012	-128	-17.2	10.1
9020500	WCR	STREAMFLOW	6/15/2012	-117	-16.3	13.4
9020500	WCR	STREAMFLOW	7/10/2012	-122	-16.7	11.6
9020500	WCR	STREAMFLOW	8/17/2012	-122	-15.4	1.20
9020500	WCR	STREAMFLOW	11/3/2012	-126	-16.6	6.80
9022000	FRUS	STREAMFLOW	10/9/2011	-131	-17.9	12.2
9022000	FRUS	STREAMFLOW	10/9/2011	-131	-17.9	12.2
9022000	FRUS	SNOW	4/29/2012	-138	-18.6	10.8
9022000	FRUS	GROUNDWATER	4/29/2012	-102	-14.0	10.0
9022000	FRUS	GROUNDWATER	4/29/2012	-107	-16.5	25.0
9022000	FRUS	GROUNDWATER	4/29/2012	-110	-14.0	2.00
9022000	FRUS	GROUNDWATER	4/29/2012	-109	-14.1	3.80
9022000	FRUS	STREAMFLOW	4/29/2012	-136	-18.6	12.8
9022000	FRUS	RAIN	5/15/2012	-60.2	-10.3	22.2
9022000	FRUS	STREAMFLOW	5/15/2012	-130	-18.6	18.7
9022000	FRUS	RAIN	6/15/2012	-101	-14.7	16.6
9022000	FRUS	STREAMFLOW	6/15/2012	-132	-17.6	8.80

USGS #	Location	Sample Type	Sampling Date	δ^2H	$\delta^{18}O$	d-*excess* (‰)
9022000	FRUS	RAIN	7/11/2012	-46.0	-7.70	15.6
9022000	FRUS	STREAMFLOW	7/11/2012	-130	-17.6	10.8
9022000	FRUS	RAIN	8/18/2012	-21.0	-4.20	12.6
9022000	FRUS	STREAMFLOW	8/18/2012	-124	-16.2	5.60
9022000	FRUS	RAIN	11/4/2012	-70.0	-9.90	9.20
9022000	FRUS	STREAMFLOW	11/4/2012	-124	-16.2	5.60
9024000	FRWP	SNOW	4/1/2012	-139	-19.7	18.6
9024000	FRWP	GROUNDWATER	4/1/2012	-128	-14.3	-13.6
9024000	FRWP	GROUNDWATER	4/1/2012	-122	-13.6	-13.2
9024000	FRWP	STREAMFLOW	4/1/2012	-128	-17.8	14.4
9024000	FRWP	GROUNDWATER	4/29/2012	-125	-15.2	-3.40
9024000	FRWP	STREAMFLOW	4/29/2012	-131	-19.6	25.8
9024000	FRWP	STREAMFLOW	5/15/2012	-129	-16.9	6.00
9024000	FRWP	STREAMFLOW	6/15/2012	-131	-17.2	6.60
9024000	FRWP	STREAMFLOW	7/11/2012	-128	-17.5	12.0
9024000	FRWP	STREAMFLOW	8/18/2012	-125	-16.7	8.60
9024000	FRWP	STREAMFLOW	11/4/2012	-125	-15.1	-4.20
9026500	SLC	STREAMFLOW	10/9/2011	-132	-17.5	8.00
9026500	SLC	STREAMFLOW	11/13/2011	-133	-17.9	10.2
9026500	SLC	STREAMFLOW	11/13/2011	-134	-17.9	9.20
9026500	SLC	SNOW	1/22/2012	-154	-20.9	13.2
9026500	SLC	SNOW	1/22/2012	-152	-20.7	13.6
9026500	SLC	SNOW	1/22/2012	-152	-20.7	13.6
9026500	SLC	SNOW	4/1/2012	-126	-17.0	10.0
9026500	SLC	SNOW	4/1/2012	-135	-19.3	19.8
9026500	SLC	GROUNDWATER	4/1/2012	-135	-16.2	-5.40
9026500	SLC	GROUNDWATER	4/1/2012	-133	-17.2	4.60
9026500	SLC	STREAMFLOW	4/1/2012	-131	-17.9	12.2
9026500	SLC	GROUNDWATER	4/29/2012	-132	-16.6	0.80
9026500	SLC	STREAMFLOW	4/29/2012	-129	-18.7	20.6
9026500	SLC	RAIN	5/15/2012	-45.7	-8.00	18.3
9026500	SLC	STREAMFLOW	5/15/2012	-129	-16.7	4.90
9026500	SLC	RAIN	6/15/2012	-95.0	-13.7	14.6
9026500	SLC	STREAMFLOW	6/15/2012	-133	-17.4	6.20
9026500	SLC	RAIN	7/11/2012	-42.0	-6.00	6.00
9026500	SLC	STREAMFLOW	7/11/2012	-128	-17.0	8.00
9026500	SLC	RAIN	8/18/2012	-16.0	-2.70	5.60
9026500	SLC	STREAMFLOW	8/18/2012	-127	-16.2	2.60
9026500	SLC	RAIN	11/4/2012	-74.0	-10.5	10.0
9026500	SLC	STREAMFLOW	11/4/2012	-126	-16.2	3.60
9032000	RCF	STREAMFLOW	10/9/2011	-127	-17.1	9.80

USGS #	Location	Sample Type	Sampling Date	δ^2H	$\delta^{18}O$	d-*excess* (‰)
9032000	RCF	STREAMFLOW	10/9/2011	-127	-16.7	6.60
9032000	RCF	STREAMFLOW	10/9/2011	-128	-17.4	11.2
9032000	RCF	SNOW	4/1/2012	-139	-19.4	16.2
9032000	RCF	GROUNDWATER	4/1/2012	-126	-15.0	-6.00
9032000	RCF	GROUNDWATER	4/1/2012	-129	-14.3	-14.6
9032000	RCF	STREAMFLOW	4/1/2012	-129	-17.5	11.0
9032000	RCF	GROUNDWATER	4/29/2012	-102	-11.7	-8.40
9032000	RCF	STREAMFLOW	4/29/2012	-127	-19.2	26.6
9032000	RCF	STREAMFLOW	5/15/2012	-122	-17.2	15.3
9032000	RCF	STREAMFLOW	6/15/2012	-124	-15.8	2.40
9032000	RCF	STREAMFLOW	7/11/2012	-121	-16.4	10.2
9032000	RCF	STREAMFLOW	8/18/2012	-119	-15.6	5.80
9032000	RCF	STREAMFLOW	11/4/2012	-119	-15.6	5.80
9032100	CC	STREAMFLOW	10/9/2011	-122	-16.6	10.8
9032100	CC	STREAMFLOW	11/13/2011	-126	-16.9	9.70
9032100	CC	SNOW	4/1/2012	-141	-19.3	13.4
9032100	CC	GROUNDWATER	4/1/2012	-131	-18.0	13.0
9032100	CC	STREAMFLOW	4/1/2012	-131	-18.9	20.2
9032100	CC	SNOW	4/29/2012	-137	-19.8	21.4
9032100	CC	GROUNDWATER	4/29/2012	-130	-17.2	7.60
9032100	CC	GROUNDWATER	4/29/2012	-130	-16.9	5.20
9032100	CC	STREAMFLOW	4/29/2012	-128	-18.9	23.2
9032100	CC	RAIN	5/15/2012	-61.3	-11.1	27.5
9032100	CC	STREAMFLOW	5/15/2012	-124	-17.6	17.3
9032100	CC	RAIN	6/15/2012	-92.0	-13.3	14.4
9032100	CC	STREAMFLOW	6/15/2012	-122	-16.4	9.20
9032100	CC	RAIN	7/11/2012	-50.0	-7.40	9.20
9032100	CC	STREAMFLOW	7/11/2012	-119	-16.3	11.4
9032100	CC	RAIN	8/18/2012	-21.0	-3.50	7.00
9032100	CC	STREAMFLOW	8/18/2012	-116	-15.5	8.00
9032100	CC	RAIN	11/4/2012	-71.0	-9.90	8.20
9032100	CC	STREAMFLOW	11/4/2012	-113	-14.9	6.20
9033100	RCT	STREAMFLOW	10/9/2011	-127	-16.8	7.40
9033100	RCT	SNOW	4/1/2012	-127	-17.4	12.2
9033100	RCT	GROUNDWATER	4/1/2012	-129	-16.5	3.00
9033100	RCT	GROUNDWATER	4/1/2012	-132	-16.2	-2.40
9033100	RCT	STREAMFLOW	4/1/2012	-130	-18.0	14.0
9033100	RCT	GROUNDWATER	4/29/2012	-125	-15.7	0.60
9033100	RCT	STREAMFLOW	4/29/2012	-127	-17.1	9.80
9033100	RCT	STREAMFLOW	4/29/2012	-129	-17.1	7.80
9033100	RCT	STREAMFLOW	5/15/2012	-121	-17.2	16.5

USGS #	Location	Sample Type	Sampling Date	δ^2H	$\delta^{18}O$	d-*excess* (‰)
9033100	RCT	STREAMFLOW	6/15/2012	-126	-16.0	2.00
9033100	RCT	STREAMFLOW	7/11/2012	-117	-15.5	7.00
9033100	RCT	STREAMFLOW	8/18/2012	-116	-14.7	1.60
9033100	RCT	STREAMFLOW	11/4/2012	-117	-14.7	0.60
9035700	WFDC	STREAMFLOW	10/8/2011	-133	-18.3	13.4
9035700	WFDC	STREAMFLOW	10/8/2011	-134	-18.3	12.4
9035700	WFDC	STREAMFLOW	11/12/2011	-134	-17.8	8.40
9035700	WFDC	SNOW	3/31/2012	-130	-17.5	10.0
9035700	WFDC	STREAMFLOW	3/31/2012	-130	-17.7	11.6
9035700	WFDC	GROUNDWATER	4/28/2012	-125	-15.7	0.60
9035700	WFDC	GROUNDWATER	4/28/2012	-132	-16.2	-2.40
9035700	WFDC	GROUNDWATER	4/28/2012	-131	-15.8	-4.60
9035700	WFDC	STREAMFLOW	4/28/2012	-132	-17.5	8.00
9035700	WFDC	STREAMFLOW	5/14/2012	-126	-17.7	15.2
9035700	WFDC	STREAMFLOW	6/15/2012	-128	-16.8	6.40
9035700	WFDC	STREAMFLOW	7/10/2012	-125	-17.4	14.2
9035700	WFDC	STREAMFLOW	8/17/2012	-127	-16.4	4.20
9035700	WFDC	STREAMFLOW	11/3/2012	-128	-16.5	4.00
9035900	SFWF	STREAMFLOW	10/8/2011	-132	-18.5	16.0
9035900	SFWF	STREAMFLOW	11/12/2011	-136	-18.6	12.4
9035900	SFWF	SNOW	1/21/2012	-142	-19.6	14.8
9035900	SFWF	SNOW	1/21/2012	-142	-19.6	14.8
9035900	SFWF	STREAMFLOW	1/21/2012	-137	-18.3	9.40
9035900	SFWF	SNOW	3/31/2012	-142	-18.7	7.60
9035900	SFWF	GROUNDWATER	3/31/2012	-109	-12.0	-13.0
9035900	SFWF	GROUNDWATER	3/31/2012	-110	-12.4	-10.8
9035900	SFWF	STREAMFLOW	3/31/2012	-136	-17.8	6.40
9035900	SFWF	GROUNDWATER	4/28/2012	-128	-15.7	-2.40
9035900	SFWF	STREAMFLOW	4/28/2012	-133	-17.9	10.2
9035900	SFWF	RAIN	5/14/2012	-59.9	-9.00	12.1
9035900	SFWF	STREAMFLOW	5/14/2012	-132	-17.7	10.1
9035900	SFWF	RAIN	6/15/2012	-81.0	-10.7	4.60
9035900	SFWF	STREAMFLOW	6/15/2012	-130	-17.4	9.20
9035900	SFWF	RAIN	7/10/2012	-40.0	-5.90	7.20
9035900	SFWF	STREAMFLOW	7/10/2012	-129	-17.6	11.8
9035900	SFWF	RAIN	8/17/2012	-16.0	-2.80	6.40
9035900	SFWF	STREAMFLOW	8/17/2012	-127	-16.8	7.40
9035900	SFWF	RAIN	11/3/2012	-69.0	-9.90	10.2
9035900	SFWF	STREAMFLOW	11/3/2012	-130	-16.1	-1.20
9036000	WFL	STREAMFLOW	10/8/2011	-133	-17.8	9.40
9036000	WFL	SNOW	3/31/2012	-126	-16.2	3.60

USGS #	Location	Sample Type	Sampling Date	δ^{2}H	δ^{18}O	d-*excess* (‰)
9036000	WFL	GROUNDWATER	3/31/2012	-128	-16.7	5.60
9036000	WFL	GROUNDWATER	3/31/2012	-131	-17.1	5.80
9036000	WFL	STREAMFLOW	3/31/2012	-132	-16.7	1.60
9036000	WFL	GROUNDWATER	4/28/2012	-134	-17.3	4.40
9036000	WFL	STREAMFLOW	4/28/2012	-132	-18.1	12.8
9036000	WFL	STREAMFLOW	5/14/2012	-131	-17.5	9.50
9036000	WFL	STREAMFLOW	6/15/2012	-129	-17.1	7.80
9036000	WFL	STREAMFLOW	7/10/2012	-129	-16.8	5.40
9036000	WFL	STREAMFLOW	8/17/2012	-128	-16.9	7.20
9036000	WFL	STREAMFLOW	11/3/2012	-130	-16.4	1.20
9037500	WFP	STREAMFLOW	11/12/2011	-133	-17.5	7.50
9037500	WFP	STREAMFLOW	1/21/2012	-135	-18.2	10.6
9037500	WFP	GROUNDWATER	3/31/2012	-96.0	-13.0	8.00
9037500	WFP	GROUNDWATER	3/31/2012	-132	-16.6	0.80
9037500	WFP	STREAMFLOW	3/31/2012	-132	-17.1	4.80
9037500	WFP	GROUNDWATER	4/28/2012	-114	-13.9	-2.80
9037500	WFP	GROUNDWATER	4/28/2012	-120	-14.8	-1.60
9037500	WFP	STREAMFLOW	4/28/2012	-125	-17.7	16.6
9037500	WFP	STREAMFLOW	5/14/2012	-129	-16.9	6.70
9037500	WFP	STREAMFLOW	6/15/2012	-129	-16.7	4.60
9037500	WFP	STREAMFLOW	7/10/2012	-126	-17.3	12.4
9037500	WFP	STREAMFLOW	8/17/2012	-123	-15.9	4.20
9037500	WFP	STREAMFLOW	11/3/2012	-127	-15.9	0.20
9047500	SR	STREAMFLOW	11/12/2011	-131	-17.3	7.00
9047500	SR	SNOW	1/21/2012	-169	-22.1	7.80
9047500	SR	SNOW	1/21/2012	-170	-22.1	6.80
9047500	SR	STREAMFLOW	1/21/2012	-128	-17.7	13.6
9047500	SR	SNOW	3/31/2012	-145	-19.2	8.60
9047500	SR	STREAMFLOW	3/31/2012	-134	-17.9	9.20
9047500	SR	GROUNDWATER	4/28/2012	-119	-15.1	1.80
9047500	SR	GROUNDWATER	4/28/2012	-121	-14.5	-5.00
9047500	SR	GROUNDWATER	4/28/2012	-121	-14.8	-2.60
9047500	SR	STREAMFLOW	4/28/2012	-131	-19.2	22.6
9047500	SR	STREAMFLOW	5/14/2012	-126	-17.2	12.1
9047500	SR	STREAMFLOW	6/15/2012	-125	-16.7	8.60
9047500	SR	STREAMFLOW	7/11/2012	-128	-17.1	8.80
9047500	SR	STREAMFLOW	8/18/2012	-120	-15.8	6.40
9047500	SR	STREAMFLOW	11/4/2012	-121	-15.1	-0.20
9047700	KG	STREAMFLOW	11/12/2011	-135	-17.8	7.90
9047700	KG	SNOW	1/21/2012	-174	-22.6	6.80
9047700	KG	SNOW	1/21/2012	-173	-22.8	9.40

USGS #	Location	Sample Type	Sampling Date	δ^2H	$\delta^{18}O$	d-*excess* (‰)
9047700	KG	STREAMFLOW	1/21/2012	-137	-18.0	7.00
9047700	KG	SNOW	3/31/2012	-141	-18.2	4.60
9047700	KG	GROUNDWATER	3/31/2012	-96.0	-10.7	-10.4
9047700	KG	GROUNDWATER	3/31/2012	-122	-13.7	-12.4
9047700	KG	STREAMFLOW	3/31/2012	-135	-17.4	4.20
9047700	KG	GROUNDWATER	4/28/2012	-123	-14.4	-7.80
9047700	KG	STREAMFLOW	4/28/2012	-132	-19.8	26.4
9047700	KG	RAIN	5/14/2012	-72.9	-10.7	12.7
9047700	KG	STREAMFLOW	5/14/2012	-128	-17.3	10.2
9047700	KG	RAIN	6/15/2012	-102	-14.0	10.0
9047700	KG	STREAMFLOW	6/15/2012	-127	-16.6	5.80
9047700	KG	RAIN	7/11/2012	-48.0	-7.80	14.4
9047700	KG	STREAMFLOW	7/11/2012	-130	-17.4	9.20
9047700	KG	RAIN	8/18/2012	-17.0	-2.90	6.20
9047700	KG	STREAMFLOW	8/18/2012	-128	-16.5	4.00
9047700	KG	RAIN	11/4/2012	-62.0	-8.40	5.20
9050100	TC	STREAMFLOW	11/12/2011	-130	-17.3	8.50
9050100	TC	SNOW	1/21/2012	-163	-21.5	9.00
9050100	TC	SNOW	1/21/2012	-164	-21.6	8.80
9050100	TC	STREAMFLOW	1/21/2012	-132	-17.4	7.20
9050100	TC	SNOW	3/31/2012	-137	-17.5	3.00
9050100	TC	SNOW	3/31/2012	-141	-18.3	5.40
9050100	TC	GROUNDWATER	3/31/2012	-114	-14.5	2.00
9050100	TC	STREAMFLOW	3/31/2012	-135	-17.9	8.20
9050100	TC	GROUNDWATER	4/28/2012	-129	-16.0	-1.00
9050100	TC	GROUNDWATER	4/28/2012	-132	-16.4	-0.80
9050100	TC	STREAMFLOW	4/28/2012	-132	-19.0	20.0
9050100	TC	STREAMFLOW	5/14/2012	-127	-16.5	4.70
9050100	TC	STREAMFLOW	6/15/2012	-126	-16.5	6.00
9050100	TC	STREAMFLOW	7/11/2012	-128	-17.3	10.4
9050100	TC	STREAMFLOW	8/17/2012	-121	-15.9	6.20
9050100	TC	STREAMFLOW	11/3/2012	-124	-15.6	0.80
9051050	SC	STREAMFLOW	11/12/2011	-137	-18.0	7.50
9051050	SC	STREAMFLOW	11/12/2011	-137	-18.2	8.60
9051050	SC	SNOW	1/21/2012	-164	-21.3	6.40
9051050	SC	SNOW	1/21/2012	-165	-21.1	3.80
9051050	SC	STREAMFLOW	1/21/2012	-139	-18.8	11.4
9051050	SC	STREAMFLOW	3/31/2012	-137	-18.1	7.80
9051050	SC	GROUNDWATER	4/28/2012	-115	-12.2	-17.4
9051050	SC	GROUNDWATER	4/28/2012	-138	-17.6	2.80
9051050	SC	GROUNDWATER	4/28/2012	-124	-13.0	-20.0

USGS #	Location	Sample Type	Sampling Date	δ^{2}H	δ^{18}O	d-*excess* (‰)
9051050	SC	STREAMFLOW	4/28/2012	-137	-20.5	27.0
9051050	SC	RAIN	5/14/2012	-74.3	-9.80	4.10
9051050	SC	STREAMFLOW	5/14/2012	-131	-17.0	5.20
9051050	SC	RAIN	6/15/2012	-97.0	-13.9	14.2
9051050	SC	STREAMFLOW	6/15/2012	-132	-17.0	4.00
9051050	SC	RAIN	7/11/2012	-43.0	-6.20	6.60
9051050	SC	STREAMFLOW	7/11/2012	-133	-18.6	15.8
9051050	SC	RAIN	8/18/2012	-20.0	-3.40	7.20
9051050	SC	STREAMFLOW	8/18/2012	-131	-17.0	5.00
9051050	SC	RAIN	11/4/2012	-64.0	-9.10	8.80
9051050	SC	STREAMFLOW	11/4/2012	-131	-16.2	-1.40
9061600	EFER	SNOW	3/31/2012	-159	-21.6	13.8
9061600	EFER	GROUNDWATER	3/31/2012	-140	-19.7	17.6
9061600	EFER	STREAMFLOW	3/31/2012	-137	-18.7	12.6
9061600	EFER	GROUNDWATER	4/28/2012	-95.0	-12.0	1.00
9061600	EFER	GROUNDWATER	4/28/2012	-117	-15.3	5.40
9061600	EFER	STREAMFLOW	4/28/2012	-136	-19.9	23.2
9061600	EFER	STREAMFLOW	5/14/2012	-132	-17.3	6.00
9061600	EFER	RAIN	6/16/2012	-90.0	-12.7	11.6
9061600	EFER	STREAMFLOW	6/16/2012	-132	-17.1	4.80
9061600	EFER	RAIN	8/17/2012	-26.0	-4.10	6.80
9061600	EFER	STREAMFLOW	8/17/2012	-124	-16.2	5.60
9061600	EFER	RAIN	11/3/2012	-79.0	-12.0	17.0
9061600	EFER	STREAMFLOW	11/3/2012	-125	-15.7	0.60
9065500	GC	GROUNDWATER	3/31/2012	-120	-15.0	0.00
9065500	GC	GROUNDWATER	3/31/2012	-134	-16.4	-2.80
9065500	GC	STREAMFLOW	3/31/2012	-129	-17.5	11.0
9065500	GC	SNOW	4/28/2012	-131	-18.5	17.0
9065500	GC	GROUNDWATER	4/28/2012	-137	-17.7	4.60
9065500	GC	STREAMFLOW	4/28/2012	-129	-19.2	24.6
9065500	GC	RAIN	5/14/2012	-62.0	-8.50	6.00
9065500	GC	STREAMFLOW	5/14/2012	-122	-16.3	8.10
9065500	GC	STREAMFLOW	5/14/2012	-124	-16.1	4.80
9065500	GC	RAIN	6/16/2012	-93.0	-13.9	18.2
9065500	GC	STREAMFLOW	6/16/2012	-127	-18.4	20.2
9065500	GC	RAIN	7/11/2012	-48.0	-7.80	14.4
9065500	GC	STREAMFLOW	7/11/2012	-123	-16.4	8.20
9065500	GC	RAIN	8/17/2012	-22.0	-3.40	5.20
9065500	GC	STREAMFLOW	8/17/2012	-110	-14.1	2.80
9065500	GC	RAIN	11/3/2012	-66.0	-9.10	6.80
9065500	GC	STREAMFLOW	11/3/2012	-113	-14.5	3.00

USGS #	Location	Sample Type	Sampling Date	δ^2H	$\delta^{18}O$	d-*excess* (‰)
9066200	BC	GROUNDWATER	3/31/2012	-124	-15.5	0.00
9066200	BC	GROUNDWATER	3/31/2012	-110	-13.2	-4.40
9066200	BC	STREAMFLOW	3/31/2012	-130	-18.0	14.0
9066200	BC	GROUNDWATER	4/28/2012	-134	-17.2	3.60
9066200	BC	STREAMFLOW	4/28/2012	-129	-18.9	22.2
9066200	BC	STREAMFLOW	5/14/2012	-126	-17.1	11.2
9066200	BC	STREAMFLOW	6/16/2012	-124	-16.5	8.00
9066200	BC	STREAMFLOW	6/16/2012	-126	-18.1	18.8
9066200	BC	STREAMFLOW	7/11/2012	-124	-16.7	9.60
9066200	BC	STREAMFLOW	8/17/2012	-111	-15.1	9.80
9066200	BC	STREAMFLOW	11/3/2012	-110	-14.2	3.60
9066300	MC	GROUNDWATER	3/31/2012	-130	-16.0	-2.00
9066300	MC	GROUNDWATER	3/31/2012	-116	-15.8	10.4
9066300	MC	STREAMFLOW	3/31/2012	-131	-18.2	14.6
9066300	MC	GROUNDWATER	4/28/2012	-127	-14.9	-7.80
9066300	MC	STREAMFLOW	4/28/2012	-129	-18.1	15.8
9066300	MC	STREAMFLOW	5/14/2012	-126	-16.6	6.40
9066300	MC	STREAMFLOW	6/16/2012	-127	-16.6	5.80
9066300	MC	STREAMFLOW	7/11/2012	-128	-17.5	12.0
9066300	MC	STREAMFLOW	8/17/2012	-118	-15.4	5.20
9066300	MC	STREAMFLOW	11/3/2012	-120	-15.4	3.20
9067000	BCA	GROUNDWATER	3/31/2012	-111	-13.1	-6.20
9067000	BCA	GROUNDWATER	3/31/2012	-93.0	-10.8	-6.60
9067000	BCA	STREAMFLOW	3/31/2012	-129	-18.0	15.0
9067000	BCA	GROUNDWATER	4/28/2012	-118	-15.5	6.00
9067000	BCA	STREAMFLOW	4/28/2012	-127	-18.4	20.2
9067000	BCA	STREAMFLOW	5/14/2012	-126	-16.4	5.20
9067000	BCA	STREAMFLOW	6/16/2012	-124	-16.1	4.80
9067000	BCA	STREAMFLOW	7/11/2012	-128	-17.5	12.0
9067000	BCA	STREAMFLOW	8/17/2012	-113	-14.8	5.40
9067000	BCA	STREAMFLOW	11/3/2012	-119	-15.7	6.60
9067000	BCA	STREAMFLOW	11/3/2012	-119	-15.2	2.60
	WCP	SNOW	1/22/2012	-146	-19.7	11.6
	WCP	SNOW	1/22/2012	-147	-19.4	8.20
	WCP	SNOW	1/22/2012	-149	-20.2	12.6
	WCP	SNOW	1/22/2012	-149	-20.2	12.6
	WCP	SNOW	3/30/2012	-126	-16.6	6.80
	WCP	GROUNDWATER	3/30/2012	-121	-15.1	-0.20
	WCP	GROUNDWATER	4/27/2012	-124	-15.4	-0.80
	WCP	GROUNDWATER	4/27/2012	-112	-13.0	-8.00
	WCP	RAIN	6/15/2012	-100	-15.1	20.8
	WCP	RAIN	7/10/2012	-47.0	-7.40	12.2
	WCP	RAIN	8/17/2012	-37.0	-5.70	8.60
	WCP	RAIN	11/3/2012	-73.0	-10.5	11.0